2019

A COMPROMISED LIVER ALTERS PCB TOXICITY AND NUTRIENT METABOLISM

Jazmyne D. L. Barney
University of Kentucky, jazmyne.barney@uky.edu
Digital Object Identifier: https://doi.org/10.13023/etd.2019.370

STUDENT AGREEMENT:

I represent that my thesis or dissertation and abstract are my original work. Proper attribution has been given to all outside sources. I understand that I am solely responsible for obtaining any needed copyright permissions. I have obtained needed written permission statement(s) from the owner(s) of each third-party copyrighted matter to be included in my work, allowing electronic distribution (if such use is not permitted by the fair use doctrine) which will be submitted to UKnowledge as Additional File.

I hereby grant to The University of Kentucky and its agents the irrevocable, non-exclusive, and royalty-free license to archive and make accessible my work in whole or in part in all forms of media, now or hereafter known. I agree that the document mentioned above may be made available immediately for worldwide access unless an embargo applies.

I retain all other ownership rights to the copyright of my work. I also retain the right to use in future works (such as articles or books) all or part of my work. I understand that I am free to register the copyright to my work.

REVIEW, APPROVAL AND ACCEPTANCE

The document mentioned above has been reviewed and accepted by the student's advisor, on behalf of the advisory committee, and by the Director of Graduate Studies (DGS), on behalf of the program; we verify that this is the final, approved version of the student's thesis including all changes required by the advisory committee. The undersigned agree to abide by the statements above.

Jazmyne D. L. Barney, Student

Dr. Bernhard Hennig, Major Professor

Dr. Isabel Mellon, Director of Graduate Studies

A COMPROMISED LIVER ALTERS PCB TOXICITY AND NUTRIENT METABOLISM

DISSERTATION

A dissertation submitted in partial fulfillment of the requirements for the degree of Doctor of Philosophy in the College of Medicine at the University of Kentucky

By
Jazmyne D.L. Barney

Lexington, Kentucky

Director: Dr. Bernhard Hennig, Professor of Toxicology and Nutrition

Lexington, Kentucky

2019

ABSTRACT OF DISSERTATION

A COMPROMISED LIVER ALTERS PCB TOXICITY AND NUTRIENT METABOLISM

Environmental contamination is a public health concern. In particular persistent organic pollutants like Polychlorinated Biphenyls (PCBs) have been associated with multiple chronic inflammatory diseases, including non-alcoholic fatty liver disease (NAFLD). NAFLD prevalence has steadily increased and is expected to continue to rise with an estimated 25% of the world's population and 80-100 million people affected in the United States alone. Importantly, the liver is the primary site for endobiotic and xenobiotic metabolism; hence its proper function is critical for the body's response to innate and extrinsic molecules. One way to combat the deleterious effects of PCB toxicity and fatty liver disease is by increasing consumption of beverages and foods that contain beneficial bioactive nutrients, like dietary polyphenols. However, the biological properties of these dietary compounds are subject to their bioavailability which is directly dependent on the activity of the liver.

The first aim of this dissertation was to test the hypothesis that in the presence of a compromised liver, PCB-126 toxicity is altered. Indeed, hepatic and systemic PCB-126 toxicity was exacerbated in this severe liver injury mouse model with an observed increase in hepatic inflammation, systemic inflammation, and early markers of endothelial cell dysfunction. Interestingly, we also observed an increase in the novel gut-liver axis derived cardiovascular disease (CVD) marker trimethylamine-N-oxide (TMAO). Taken altogether, aim 1 proved that a compromised liver can alter PCB toxicity, with implications of the gut microbiota in disease pathology.

In aim 2 we investigated whether GTE can protect against MCD-induced hepatic toxicity and development of NAFLD. Results indicated that MCD mice exhibited severe liver injury and gut dysbiosis and unexpectedly, GTE had no protective effects. Interestingly MCD mice displayed differential epigallocatechin-3-gallate (EGCG) metabolism at the hepatic and gut microbiota level, which may

alter polyphenol bioavailability and therapeutic potential. Overall, the results provide insight into how a dysfunctional liver and gut dysbiosis can alter polyphenol metabolism, possibly reducing its therapeutic efficiency.

In aim 3 we sought to determine potential protective effects of a prebiotic in this mouse model. MCD-fed mice were exposed to PCB-126 with or without inulin supplementation. Although findings from this study are preliminary, our evidence indicates that inulin restores body weight and body composition in this MCD+PCB mouse model and alters the expression of Cyp1a1 in PCB exposed mice, suggesting that inulin's protective effects may be a result of its ability to interact with the AhR pathway. However further analysis will need to be done to examine the effects of inulin on hepatic, systemic, and gut microbiota endpoints.

Overall the data contained in this dissertation suggests that in the presence of a compromised liver both pollutant toxicity and nutrient metabolism are altered, with implications of the gut-microbiota in disease risk. These findings suggest that individuals with end stage liver injury may be more susceptible to pollutant-induced toxicity and nutritional intervention may be unsuccessful at mitigating disease risk.

KEYWORDS: NAFLD, Gut Microbiota, PCBs, Green Tea, Inulin, Metabolism

Jazmyne D.L. Barney

07/12/2019

A COMPROMISED LIVER ALTERS PCB TOXICITY AND NUTRIENT METABOLISM

By

Jazmyne D.L. Barney

Dr. Bernhard Hennig

Director of Dissertation

Dr. Isabel Mellon

Director of Graduate Studies

07/12/2019

Date

DEDICATION

To my beautiful sister Jaliyah and my lovely granny Barbara Jean. I will forever miss you both and wish you could be here to see me get my PhD. To my unborn child Saniyah Elizabeth, thank you for keeping me sane and reminding me to keep moving forward, even during the hardest of times.

ACKNOWLEDGMENTS

First and foremost I have to thank God for getting me through this journey and finally for this honor of becoming a doctor. It is because of your goodness and my faith in you that I am here today.

I would not be in this position if it wasn't for the help of so many people. First I would like to thank my mentor Dr. Bernie Hennig for all of the support and encouragement through my tenure. He supported my academic and professional dreams in ways a typical P.I. would not and always advocated for me when I needed him to. I also have to thank Dr. Banrida Wahlang for taking me under her wing and teaching me everything she knows about being a scientist. Also the Hennig lab (Dr. Mike Petriello, Dr. Jessie Hoffman, Dr. Pan Deng, and Dr. Chunyan Wang), thank you so much for all the help and friendships. Without your collaborations and you all constantly pushing me to be greater, I would not be here today. I would also like to thank my amazing committee members Dr. Kevin Pearson, Dr. Andrew Morris, Dr. Hollie Swanson, and Dr. Xianglin Shi for being my voice and challenging me as a scientist and an individual. Thank you also to the Department of Toxicology and the UK Superfund Research Center for the opportunity to be a student and trainee for the past 4 years.

To all of my countless friends, thank you for all the encouragement through the years. From the study parties to the margarita and food dates lol thank you for helping me in so many ways. I can't name you all but you know who you are ☺

To my physical family, I can't begin to thank you enough. From day one I always felt motivated because of your love and constant support. Without you all I would have failed, so thank you. To my church family, I cannot begin to thank you for the countless prayers, spiritual guidance, and love you have shown me and my family. Through good and bad times I'm grateful to have you all in my corner.

To my grandmother, who was my rock! You knew nothing about PCRs or toxicology, but you made an effort to ask me every day about my research. To my sister who I still can't believe is no longer on this Earth. Thank you for allowing me to be your big sister, (and your mom at times). I will miss you both and am doing this for you two.

Lastly to my amazing, wonderful, faithful, and supportive husband Brian. You have been there with me every single step of this journey. From pulling me out of the closet and praying with me the day of my qualifying exam (rough times lol) to knowing the key to my heart and feeding me my favorite foods when I had to study, you were there. I literally would not be standing here saying I am a doctor without you by my side. God knew I needed you, and now Saniyah, to get through. Thank you and I love you with all of my heart.

-Jazmyne

TABLE OF CONTENTS

List of Figures

List of Tables

List of Abbreviations

Abcc1/Mrp1: ATP-binding cassette sub-family C member 2/ multidrug resistance-associated protein 1

Abcc2/Mrp2: ATP-binding cassette sub-family C member 2/ multidrug resistance-associated protein 2

AhR: aryl hydrocarbon receptor

ALT: alanine transaminase

ARNT: aryl hydrocarbon receptor nuclear translocator

AST: aspartate transaminase

BW: body weight

CAR: constitutive androstane receptor

CD: control diet

Comt: catechol-O-methyltransferase

CVD: cardiovascular diseases

Cyp1a1: cytochrome P450 1A1

Cyp1a2: cytochrome P450 1A2

EC: epicatechin

ECG: epicatechin-3-gallate

EDTA: ethylenediaminetetraacetic acid

EGC: epigallocatechin

EGCG: epigallocatechin-3-gallate

FB: Firmicutes/Bacteroidetes

FMO3: flavin-containing monooxygenase 3

GTE: green tea extract

H&E: hematoxylin and eosin

HFD: high-fat diet

hs-CRP: high-sensitive C-reactive protein

Icam-1: intercellular adhesion molecule 1

IL-6: interleukin-6

LW: liver weight

MCD: methionine-choline deficient

MCP/Ccl-2: macrophage chemoattractant protein-1/ chemokine (C-C motif) ligand 2

NAFLD: non-alcoholic fatty liver disease

NASH: non-alcoholic steatohepatitis

PAI-1: plasminogen activator inhibitor-1

PCB: polychlorinated biphenyl

Pecam-1: platelet endothelial cell adhesion molecule

POPs: persistent organic pollutants

proMMP-9: matrix metallopeptidase 9

PXR: pregnane X receptor

ROS: reactive oxygen species

SAM: S-adenosylmethionine

SCFAs: short chain fatty acids

Sult1a1: sulfotransferase family 1a member 1

Sult1b1: sulfotransferase family 1b member 1

TAFLD: toxicant-associated fatty liver disease

TASH: toxicant-associated steatohepatitis

TCDD: 2,3,7,8- tetrachlorodibenzo-p-dioxin

Timp-1: tissue inhibitor of metalloproteinases-1

TMA: trimethylamine

TMAO: trimethylamine N-oxide

TNF-α: tumor necrosis factor-α

Ugt1a1: UDP-glucuronosyltransferase 1-1

VLDL: very-low-density lipoprotein

XRE: xenobiotic response elements

Chapter 1: Introduction

Chronic inflammatory diseases

Chronic inflammatory diseases are a national health burden and currently affect millions of people globally. Although the human body naturally uses inflammatory mechanisms for tissue and wound healing, chronic inflammation can have detrimental effects. Inflammatory diseases can take form in different organs of the body including in the adipose tissue causing obesity, in the heart contributing to coronary artery diseases like atherosclerosis, in the gut resulting in illnesses such as inflammatory bowel disease and the more recently studied gut dysbiosis, or even in the liver causing fatty liver diseases and hepatic cancers [1-5]. One important notion to consider is that each of these chronic inflammatory diseases can be a risk factor for another, allowing for increased risk of developing multiple diseases in many individuals. One such disease that has been implicated as a risk factor for many others and that is becoming a global public health concern is non-alcoholic fatty liver disease (NAFLD).

Non-alcoholic fatty liver disease (NAFLD)

NAFLD is a major public health problem and the most common chronic liver disease as its prevalence has steadily increased, representing over 75% of the chronic liver disease cases, and is expected to continue to rise [6]. An estimated 25% of the world's population and 80-100 million people affected in the United States alone are suffering from the disease with the current medical and societal costs estimated at $292 billion a year [7-9]. NAFLD is the hepatic

manifestation of metabolic syndrome and is characterized as a spectrum of progressive liver diseases that is produced in the absence of severe alcohol consumption. The incidence of this disease has increased with the growing sedentary population, suggesting that lifestyle choices including poor diet and lack of exercise are major contributors to the development of NAFLD. In fact, a significant risk factor for NAFLD progression and development is being obese [10]. Risk factors in addition to obesity that also contribute to the development of NAFLD include type 2 diabetes, insulin resistance, and dyslipidemia, all of which are hallmarks of metabolic syndrome [11]. NAFLD is histologically defined as the ectopic accumulation of lipid in the hepatocytes and ranges in severity with the earliest forms being reversible. It begins with steatosis which is simple fat accumulation in the liver of greater than 5% in the hepatocytes (histologically) which can then progress to steatohepatitis which is the presence of fat and inflammation with or without fibrosis [12, 13]. Although steatosis and steatohepatitis are reversible forms of the disease, once the liver develops late stage scarring it is considered cirrhosis which is irreversible.

Although the causative mechanisms of NAFLD remains uncertain, many theories have been proposed to explain its development and progression. The “two-hit” or more recently “multiple-hit” hypothesis is the most widely accepted in the field of hepatology. This theory suggests that there is a first “hit” to the liver that initiates ectopic fat accumulation in the hepatocytes causing an imbalance in synthesis, influx, oxidation, and export of hepatic lipids [14, 15]. This increase in lipids can be a consequence of many sources including being diet-induced as a

result of the increased consumption of high caloric and fat rich foods. At this stage the liver is vulnerable to a second insult deemed the second “hit” which can be an effect produced by cytokines, oxidative stress, or gut-derived components [15].

The effects of a dysfunctional liver on drug and nutrient metabolism

It is pertinent for individuals to have a properly functioning liver since it is the chief organ responsible for the metabolism of both endogenous and exogenous substances. For this reason, multiple studies have investigated the ability of non-alcoholic steatohepatitis (NASH) to alter drug pharmacokinetics and ultimately influence the toxicity of pharmaceutical drugs. For example, Clarke et al. demonstrated that mice fed the NASH producing MCD diet exhibited alterations in metformin metabolism, causing increased risk for drug toxicity [16]. Another study in MCD-diet fed mice showed changes in the kidney, particularly the glomerular filtration and tubular secretion of the drug adefovir, causing alterations in the pharmacokinetics [17]. This is an important concept since not only can a dysfunctional liver alter drug metabolism, but similar effects can be seen with other endogenous components like pollutants and possibly beneficial nutrients [18, 19].

The Gut-Liver Axis

As stated above, the liver is the major site for endogenous and exogenous metabolism, hence a healthy and properly functioning liver is crucial to overall

host health. With regard to the liver, a critical feature to take into account is that the liver has a rich blood supply and is able to interact with multiple organs in the body. This cross-talk is crucial to understanding the development and progression of multiple disease states and studies focused on this has become a prevalent area of research across all fields over recent years. For example, NAFLD has been implicated in the perturbation of the gut microbiota in both rodent models and in human studies as seen by alterations at the phyla and genus level of microbes [20, 21]. Recent literature has indicated that the gut microbiota participates in a co-partnership with the liver, dubbed the gut-liver axis, and has an impact on the pathology of multiple chronic inflammatory diseases including NAFLD [22]. For example J. Henao-Mejia, et al. showed that mice fed a MCD diet developed a NASH phenotype which was associated with changes in the composition of the gut [23]. On the other hand, gut dysbiosis can also contribute to NAFLD by influencing the regulation of energy homeostasis, modulation of bile acid synthesis, and formation of pro-inflammatory toxins that target distant organs like the liver [22].

The Gut Microbiota

The gut microbiota is an organ with a diverse microbe population weighing in at about 2 kg that resides in the gastrointestinal tract of the host. It plays a major role in overall host health by aiding in digestion, contributing to metabolism of dietary and host-derived molecules, combating other microorganism, and acting as a first line of defense to the external environment [21]. Multiple

elements shape the identity and composition of the gut microbiota. Some examples includes the mode of birth of a newborn fetus, the age of a person, exposure to environmental contaminants, the use of antibiotics, and lifestyle choices such as diet and exercise [24-27]. Additionally, since the primary route of exposure to many pollutants is via oral intake of food and water, the gut microbiota's location makes it not only at great risk to be affected by these pollutants, but also makes it susceptible to dietary manipulation. In fact, Petriello and Hoffman et al. showed that exposure to the environmental pollutant polychlorinated biphenyl 126 (PCB-126) can increase intestinal inflammation and disrupt gut microbiota homeostasis in an atherogenic mouse model [28]. Still, ongoing research is making strides to try and identify techniques to prevent and reduce disease risk utilizing nutritional therapeutics targeting the gut microbiota [29, 30]. The gut microbiota also plays a huge role in host metabolism and energy regulation, allowing it to influence overall host health and disease outcomes in a major way. A healthy gut contains a diverse population of microbes and an imbalance of the intestinal bacteria, known as gut dysbiosis, is associated with disease development including metabolic disorders, atherosclerosis, and NAFLD [31].

Environmental pollutants and disease

The effects of exposure to environmental contamination impact almost every living population throughout the world. This is because environmental pollutants have been linked to a variety of disease outcomes and the

pathogenesis of numerous inflammatory diseases. There are multiple routes of exposure that can contribute to the increased body burden of environmental contaminates, with the most significant exposure sources being dermal, inhalation, and oral [32, 33]. Although we can encounter pollutants through all of the before mentioned routes, one of the primary ways that persons come into contact with pollutants is via the oral route, usually by accidental ingestion through contaminated food and water sources. At the cellular level pollutants exert their actions by various signaling pathways, depending on the concentration present in the cell and the cell type it effects.

NAFLD and environmental pollutants

The progression of fatty liver disease and related metabolic dysfunctions have historically been linked to an imbalance in energy intake and expenditure. However, recent epidemiological studies have shown an association of exposure to environmental pollutants, such as PCBs with the induction or exacerbation of several chronic inflammatory and metabolic diseases including obesity, cardiovascular disease, diabetes, and liver disease [34-38]. Toxicant-associated fatty liver disease (TAFLD) and the more severe form toxicant-associated steatohepatitis (TASH) has become an important field of study, relating environmental and occupational exposures to pollutants like PCBs and vinyl chloride respectively with the development of fatty liver disease [35, 39, 40].

NAFLD and Polychlorinated Biphenyls (PCBs)

More specifically, PCBs are part of a bigger class of pollutants often referred to as persistent organic pollutants or POPs. These are typically environmental contaminants that are resistant to degradation and bind to a variety of cellular receptors initiating signaling cascades thereby creating conditions that is advantageous to disease progression. PCBs are man-made aromatic chemicals that were widely used in industrial applications until their outlaw in the United States in the 1970s and worldwide in 2001 [41]. There are over 200 PCB congeners that are categorized by their structure and the degree of chlorination, with the replacement of hydrogen with chlorine atoms in the *ortho* positions of the benzene rings creating an altered configuration. This substitution of chlorine atoms in different positions on the aromatic rings enables coplanar and non-coplanar configurations and specific interactions with regulators of detoxification, the xenobiotic cellular receptors. Coplanar, dioxin-like PCBs including PCB-126 are agonist of a transcription factor called the aryl hydrocarbon receptor (AhR) while non-coplanar, phenobarbital-like PCBs such as PCB 153 act on the constitutive androstane receptor (CAR)/pregnane X receptor (PXR) [42-44]. In addition, PCBs have high thermal stability and their hydrophobicity and resistance to metabolic degradation which allows them to biomagnify in the food chain, eventually leading to their bioaccumulation in human adipose tissue. Today, most human exposures to PCBs are through contaminated food sources, allowing for PCBs to cause disruption to several organ systems [45].

In the cytoplasm of the cell, PCB-126 binds to the AhR, causing the disassociation of chaperone proteins from the receptor and subsequent translocation to the nucleus. AhR then heterodimerizes with the co-factor aryl hydrocarbon receptor nuclear translocator (ARNT) and binds to xenobiotic response elements (XRE) in the promoter region of AhR target genes, including detoxifying enzymes such as cytochrome P450 1A1 (Cyp1A1). The chronic exposure to PCBs can lead to chronic activation of the AhR and increased expression of its downstream target genes, causing decoupling and the release of reactive oxygen species (ROS). This chronic inflammatory and oxidative stressful state is what is believed to be the mechanism by which PCBs elicits the development, progression, or exacerbation of chronic inflammatory diseases like NAFLD. For instance with regards to liver diseases like NAFLD and hepatocellular carcinoma, pollutants like 2,3,7,8- tetrachlorodibenzo-p-dioxin (TCDD) and PCB-126 can increase risk and disease severity by activating AhR, subsequently increasing hepatic and systemic inflammation [43, 44].

Rodent models of NAFLD

There are multiple rodent models that exist to investigate NAFLD and many have been used to mimic human liver disease [46]. However, choosing the right model for study is pertinent, as they all have both benefits and limitations. In particular, the highly reproducible MCD-diet mouse model has been extensively used in research to mimic human NASH. This diet typically contains a significant carbohydrate source but is deficient in both methionine and choline. Choline is a

major component of very-low-density lipoprotein (VLDL) and the lack of this nutrient leads to impaired hepatic production and secretion of lipoproteins, subsequently resulting in ectopic fat accumulation in the liver [47, 48]. Additionally, a deficiency in choline alters the mitochondrial function, producing fatty acid oxidation disturbances [49]. Methionine plays a different role in NASH development within this diet. Methionine is important for not only protein synthesis, but also the synthesis of anti-oxidant molecules such as S-adenosylmethionine (SAM) and glutathione. The absence of this essential amino acid causes hepatic methyl imbalance and oxidative stress, contributing to the development of NAFLD [50-52]. All of this is important, with choline deficiency leading to the human NAFLD phenotype while methionine deficiency promotes oxidative stress and possibly drives an inflammatory response by alterations in cytokine production [53, 54].

Moreover, the use of animal models is an important tool for investigating the molecular mechanisms that contributes to the development of diseases as a result of pollutant exposures. A benefit of using the MCD-diet model to study NASH is that when mice are fed this diet, they do not become obese and instead exhibit weight loss, producing a lean phenotype [46]. Although it is true that human NASH is closely associated with obesity using a lean mouse model is crucial when studying TASH, especially when examining the effects of lipophilic pollutants. Other popular NAFLD rodent models like high-fat diet (HFD) feeding is not the most advantageous to study these classes of pollutants because it has

been shown that obese mice are protected against the effects of lipophilic pollutants as an increase adipose stores limits pollutant bioavailability [55].

Nutritional Intervention

Even with increased effort and programs to decrease the public burden of environmental exposures and significant advancements in modern day medicine, there still remains a deficiency in the treatment of inflammatory diseases. With respect to NAFLD, the current clinical treatment for the disease is to decrease weight by 10% through decreased caloric consumption and increased exercise. Unfortunately, this method has proven difficult to maintain in practice with limited long-term success [56, 57]. Thus, a recent clinical guideline that has been suggested by clinicians and the like is increasing consumption of more nutrient rich foods to decrease or ameliorate countless inflammatory and pollutant-related diseases including diabetes, obesity, fatty liver disease, and gastrointestinal tract illnesses. One reason this therapy is so promising is that most of these pollutant-induced non-communicable diseases exert their harmful health results via signaling mechanisms associated with oxidative stress, inflammation, and carbohydrate and lipid metabolic pathways, which are the same mechanisms that many beneficial nutrients act on. Similarly, the ailments from exposure to environmental toxins like PCB-126 also results from these pollutants working through these same molecular pathways, permitting beneficial nutrition to be a promising means to contest undesirable health outcomes associated with environmental pollutant and diet-induced diseases.

Green Tea and related beneficial metabolites

One dietary intervention that has been associated with a decrease in NAFLD development and progression is increased consumption of tea. Tea is the 2nd most consumed beverage in the world just behind water and has been used for centuries as a means to combat disease. The manufacturing process of tea allows for six different classification groups: green, black, yellow, white, dark, and oolong. This difference in processing contributes to multiple properties and characteristics distinct to the class of tea such as color, taste, and aroma. In particular, green tea accounts for 20% of the world's tea consumption [58]. Moreover, green tea and its major bioactive polyphenolic catechin epigallocatechin-3-gallate (EGCG) have been well studied as a therapeutic for NAFLD using *in vitro* and *in vivo* models in recent years [59-61]. EGCG along with epigallocatechin (EGC), epicatechin-3-gallate (ECG), and epicatechin (EC) are the most abundant catechins found in green tea with EGCG accounting for 50-75% of the total catechin abundance [58, 62]. Although the exact biological effects of EGCG and other green tea polyphenols are still under investigation, it has been shown that these molecules can decrease expression of hepatic transcription factors involved in downstream inflammatory responses and increase expression of transcription factors involved in the activation of antioxidant response, resulting in anti-inflammatory and anti-oxidant properties respectively in rodent models of fatty liver disease [63, 64]. However, the

biological properties of dietary polyphenols are subject to their bioavailability which is directly dependent on the activity of the liver.

Inulin and related beneficial metabolites

Another dietary intervention that has gained interest as of late is consuming a diet that is enriched with fiber. According to the 2015-2020 Dietary Guidelines for Americans, the recommended intake amount of dietary fiber is 14 grams per 1000 calories, but unfortunately most Americans are not consuming this quantity (<3%) [65, 66]. With increasing knowledge that the gut microbiota can influence multiple disease outcomes one particular class of fiber, prebiotics, have become a huge field to study. Prebiotics are any “selectively fermented ingredient that allows specific changes, both in the composition and/or activity in the gastrointestinal microflora, that confers benefits” [67]. When fermented by the microbiota in the colon, prebiotics yield metabolites known as short chain fatty acids (SCFAs) which can be absorbed and exert systemic actions, ultimately decreasing disease risk and outcomes [68].

Recent studies have shown that a critical component of the interplay that exists between the diet and the gut-liver axis involves SCFAs [69]. In the colon, the non-digestible prebiotic inulin is predominately fermented to a handful of SCFAs, acetate (82%), butyrate (12%) and propionate (6%) [70]. With regards to NAFLD, inulin can modulate risk and outcome by exerting anti-inflammatory and anti-oxidant effects. In one study, patients with NAFLD given a pro-biotic capsule plus Inulin showed improved inflammatory and oxidative parameters such as

decreased serum tumor necrosis factor-α (Tnf-α) and high-sensitive C-reactive protein (hs-CRP), providing a possible dietary treatment for the disease [71]. A similar response was also seen in mice fed atherogenic and steatosis producing HFD. Here, supplementation with a natural dietary supplement containing inulin prevented the development of NAFLD and atherogenic lesions by modulating signaling pathways involved in lipogenesis, lipid oxidation, and inflammation [72]. These new findings suggest that prebiotic supplementation with inulin may be an effective means to treat NAFLD, although data is still lacking and the related mechanisms remains unclear.

Taking all this into account, it is clear that additional research is needed to determine the mechanisms by which pre-existing liver disease can influence the toxicity of PCBs. In addition, since modifications in diet and nutrition, such as increased consumption of green tea or prebiotic fibers, has been both historically and recently used as a therapeutic method to combat chronic inflammatory diseases and is dependent on a healthy liver, it is important to investigate to what extent can tea polyphenols and prebiotic fibers protect against the negative health effects caused by severe, end state liver disease. Hence, the objectives of this dissertation are outlined below.

Scope of Dissertation

The overall objective of this project is determine the mechanisms by which a compromised liver can worsen PCB 126 toxicity and if beneficial nutrition can attenuate these effects.

PCB-126 and the MCD diet were chosen to be utilized in the studies within this dissertation as a model pollutant and a model of severe fatty liver disease. PCB-126 has historically been implicated in negative human health effects and its structure is similar to many other pollutants, allowing for PCB-126 to be an ideal candidate for study. The MCD-diet causes the most severe stage of fatty liver disease and the mechanism by which steatosis is produced allows for ectopic fat accumulation to occur mainly in the liver, resulting in a lean mouse phenotype. These considerations are important because most liver disease studies focus on the beginning stages of liver disease when nearly 25% of those diagnosed with NAFLD eventually will present with NASH, the more severe disease phenotype [73]. Also, the effects of PCB-126 are dependent on its total body burden, with lean models possibly being more effective in studying lipophilic and dioxin-like pollutant toxicity.

Our central hypothesis is that PCB-126 toxicity is worsened in the presence of a compromised liver and that nutritional intervention (green tea extract and inulin) can ameliorate these effects. As such, we will test our central hypothesis with the following specific aims:

Specific Aim 1: Test the hypothesis that PCB-126 toxicity is worsened in the presence of a compromised liver in wild type C57BL/6 mice.

Specific Aim 2: Test the hypothesis that the polyphenol-rich green tea extract (GTE) can protect against diet-induced liver injury in wild type C57BL/6 mice.

Specific Aim 3: Test the hypothesis that the prebiotic fiber inulin can attenuate steatohepatitis and PCB-126 toxicity in wild type C57BL/6 mice.

Chapter 2 Specific Aim 1: To test the hypothesis that PCB-126 toxicity is worsened in the presence of a compromised liver in wild type C57BL/6 mice

The data contained in this chapter has been previously published and permission for re-use of select text and figures has been obtained by the first author (B. Wahlang), the corresponding author (B. Hennig), and the publisher (Oxford University Press). Please see the below citation and appendix for additional details.

Wahlang B, Barney J, Thompson B, Wang C, Hamad OM, Hoffman JB, et al. Editor's Highlight: PCB126 Exposure Increases Risk for Peripheral Vascular Diseases in a Liver Injury Mouse Model. Toxicol Sci. 2017;160:256-67. [18]

Summary

SCOPE: The liver plays a major role in overall metabolism, thus its proper function is crucial for overall health and protection against disease pathologies. Our lab has previously shown that PCB toxicity is exacerbated in mice with a dysfunctional liver. However how severe liver injury can influence PCB-126 induced toxicity on other organ systems, such as the peripheral vasculature, and its associated disease states still needs to be examined. This study sought to investigate whether a compromised liver influenced PCB-126 toxicity on vascular inflammation in mice with severe liver injury.

METHODS AND RESULTS: In this 14-week study, male C57BL/6 mice were fed either a purified amino acid control diet (CD) or a methionine-choline deficient (MCD) diet with or without PCB-126 (0.5 mg/kg) exposure. Post euthanasia, tissues were collected and analyzed for histological, inflammatory, and metabolic parameters. PCB-126 caused steatosis irrespective of diet and mice fed the MCD-diet demonstrated steatosis. However, only in the MCD+PCB-126 group did we observe the presence of steatosis and fibrosis, indicative of steatohepatitis. Interestingly, the MCD+PCB-126 mice had increased hepatic and plasma inflammatory cytokine markers including Tumor necrosis factor alpha (Tnf-α) and macrophage chemoattractant protein-1/ chemokine (C-C motif) ligand 2 (Mcp-1/Ccl-2). Interestingly, we also observed a significant increase in the hepatic and plasma levels of the proatherogenic biomarker trimethylamine-N-oxide (TMAO) providing evidence of gut microbiota-liver interactions and vascular inflammation that is typically seen in atherosclerosis.

CONCLUSIONS: The results presented in this study provides a novel link between a dysfunctional liver and PCB-126 toxicity on the liver and the peripheral vasculature, with implications of a role of the gut microbiota. This provides an important mechanistic role of dioxin-like pollutants, indicating their ability to contribute to the development and/or progression of inflammatory diseases via crosstalk with other organ systems.

Introduction

Exposure to environmental pollutants is a huge public health concern. Namely, a class of pollutants, the Polychlorinated Biphenyls (PCBs), have been implicated in many diseases states. PCBs were used predominately in industrial applications until their banishment in the 1970s in the USA and worldwide in 2001 [41]. Although the production and use was banned, PCBs still persist in the environment because of their physical and chemical properties. Additionally, the major route of exposure to these chemicals is through the oral route via ingestion of contaminated food sources [45, 74, 75].

There are over 200 different congeners of PCBs. Their structure, most importantly their degree and position of chlorination on the biphenyl rings, determines their physical and chemical properties such as whether they present as a planar or co-planar configuration, their level of toxicity, and their mechanism of action. In particular co-planar, dioxin-like PCBs like PCB-126 can bind and activate the hepatic AhR, a transcription factor that can bind to the promoter regions in genes involved in detoxification and has been correlated with the pathology of a variety of chronic inflammatory diseases including obesity, cardiovascular diseases (CVDs), and liver diseases [35, 36, 38, 43, 44, 76-78].

Since most exposures of PCBs occurs through the oral route, it is important to consider how the liver influences its detoxification and overall toxicity. The liver is also the primary site of both xenobiotic and endobiotic metabolism hence its proper function is crucial. In addition to diet, exercise, and alcohol consumption, chemical toxins also can contribute to NAFLD

development. Importantly, liver disease can increase risk for other cardiometabolic diseases such as atherosclerosis and ligand activation of the AhR has been associated with both hepatic maladies and CVDs, suggesting AhR ligands could be a possible link between liver and cardiovascular diseases [79-82]. However, the mechanisms linking the liver and the peripheral vasculature to inflammatory disease outcomes is limited [83, 84].

Taken altogether, the objective of this present study is to explore the effects that the dioxin-like, AhR ligand PCB-126 exerts on circulating inflammatory cytokines and vascular inflammation in the presence of a dysfunctional liver.

Experimental design and methods

Animals, diet, and experimental design

All procedures and tests discussed in this study was approved by the University of Kentucky Institutional Animal Care and Use Committee. Animals were housed in a light and temperature controlled room on a 12 hour light/dark cycle with food and water given ad libitum. In this 14-week study, forty eight-week old male C57Bl/6 mice were obtained from Taconic (Hudson, New York, USA) and divided into 4 experimental groups (n=10). Mice were fed either a purified amino acid control diet (CD; TD.94149; Envigo, Madison, Wisconsin, USA) or the liver injury producing methionine-choline deficient diet (MCD diet TD.90262, Envigo) and gavaged with either vehicle corn oil or PCB-126 in corn oil (0.5 mg/kg; AccuStandard, Connecticut, USA) at week 4 of the study, resulting

in the following groups (n=10): CD, CD+PCB-126, MCD, MCD+PCB-126. On week 1 of the study all mice were fed the CD and on week 2 respective groups were fed either CD or MCD diet. MCD-diet fed mice were reverted back to CD on week 5-6 of the study and then returned to MCD diet for the remainder of the study. This measure was taken to avoid excessive weight loss and subsequent noncompliance with the approved IACUC protocol. Body weight was measured weekly and liver weights were taken post euthanasia. To assess for body composition, all mice were analyzed for lean and body fat mass using the EchoMRI (EchoMRI LLC, Houston, Texas, USA) at the completion of the study.

Plasma and tissue collection

Post euthanasia blood samples were collected, placed into tubes containing ethylenediaminetetraacetic acid (EDTA), briefly mixed, and centrifuged at 2000 g for 15 min at 4 C to separate blood plasma. Plasma and tissues samples were immediately frozen in liquid nitrogen and stored at -80°C until further analysis.

Histological examination

For histological examination, liver sections were fixed in 10% neutral buffered formalin and embedded in paraffin. Hepatic sections were stained with hematoxylin and eosin (H&E) and examined by light microscopy. All reagents were obtained Sigma Aldrich Corp. (St Louis, Missouri, USA). Images were captured using a high-resolution digital scanner at 10 and 40 magnification.

Using ImageJ software (NIH, Bethesda, Maryland, USA) fibrosis quantification was performed as previously described in Hadi et al [85].

Plasma Cytokine Measurements

The Milliplex Map Mouse Adipokine Magnetic Bead Panel (Millipore Corp, Billerica, Massachusetts, USA) was used to measure plasma cytokines (tumor necrosis factor alpha (Tnf-α), interleukin-6 (IL-6), macrophage chemoattractant protein-1 [Mcp-1]), and plasminogen activator inhibitor-1 (PAI-1) while the Milliplex Map Mouse CVD Magnetic Bead Panel 1 was used to measure plasma CVD markers on the Luminex Xmap MAGPIX system (Luminex Corp, Austin, Texas, USA), following manufacturer's instructions. Plasma aspartate transaminase (AST) and alanine transaminase (ALT) activity were measured with the Piccolo Xpress Chemistry Analyzer using Lipid Panel Plus reagent disks (CLIAwaived Inc., San Diego, California, USA).

Measurement of trimethylamine-N-oxide (TMAO)

Post euthanasia, methanol and acetonitrile was used to extract trimethylamine-N-oxide (TMAO) from 10 µl of plasma and ~50 mg liver tissues and respectively. HPLC electrospray ionization tandem mass spectrometry was used to analyze TMAO as described previously with slight modifications [86, 87]. Analysis was conducted using Shimadzu HPLC coupled with an AB Sciex 6500-QTRAP hybrid linear ion trap triple quadrupole mass spectrometer in multiple reaction monitoring mode. For use as an internal standard and for relative

quantitation, mass labeled choline (d4-choline) was employed. TMAO was analyzed using a Primesep 100, 3 µm, 2.1 x 100 mm column (SIELC Technologies, Wheeling IL) and data were processed using ABSciex Multiquant software.

mRNA extraction and PCR

Total mRNA was extracted from mouse tissues samples using the TRIzol reagent (Thermo Fisher Scientific Inc., Waltham, Massachusetts, USA). The NanoDrop 2000/2000c (Thermo Fisher Scientific Inc.) using the NanoDrop 2000 (Installation Version 1.6.198) software was utilized to determine RNA purity and quantity. Next, complementary DNA was synthesized from total mRNA using the QuantiTect Reverse Transcription Kit (Qiagen, Valencia, California, USA). Polymerase chain reaction (PCR) was performed on the CFX96 Touch Real-Time PCR Detection System (Bio-Rad, Hercules, California, USA) using the Taqman Fast Advanced Master Mix (Thermo Fisher Scientific Inc.). All primers used in this study were acquired from Taqman Gene Expression Assays (Thermo Fisher Scientific Inc.). For liver gene expression the levels of mRNA were normalized relative to the amount of Actb with expressions levels of the CD+Vehicle experimental group set at 1. Gene expression levels were calculated using the $2^{-\Delta\Delta Ct}$ method [88].

Statistical analysis

All analyses were overseen by University of Kentucky biostaticians. Statistical analyses was conducted and graphs were plotted using GraphPad

Prism version 7.02 for Windows (GraphPad Software Inc., La Jolla, California, USA). Multiple group data were compared using 2-way ANOVA (column factor: diet and row factor: PCB-126) followed by Tukey's post-hoc test for multiple comparisons. $p < .05$ was considered statistically significant. All data are expressed as mean ± SEM.

Results

2.1 Experimental design

The experimental design for this study is presented in Figure 2.1.

2.2 PCB-126 Exposure Worsened Liver Injury Caused by MCD Feeding

Firstly, in an effort to determine if the presence of a compromised altered PCB-126 toxicity, we examined hepatic liver sections for steatosis, inflammation, and fibrosis. Hepatic tissue samples were stained with H&E and assessed. It was demonstrated that mice MCD diet fed mice developed severe steatosis evidenced by ectopic fat infiltration in the hepatocytes, a major hallmark of steatosis. The MCD mice also exhibited indications of steatohepatitis, shown by the presence of inflammatory foci and fibrosis, the later confirmed by representative assessment via pico-sirius red staining of hepatic sections (Figure 2.2).

To gain a better understanding of the inflammatory and fibrotic response in the liver, PCR was conducted to assess the gene expression of the inflammatory markers Mcp1 (Ccl2) and Tnf-α, and the fibrotic markers PAI-1 and tissue inhibitor of metalloproteinases-1 (Timp1) (Figure 2.2). Remarkably, the

concomitant MCD+PCB-126 group displayed increased levels of expression of Mcp-1, Tnf-α, PAI-1, and Timp-1 in the liver when compared to all other groups. Additionally, the MCD+PCB-126 group exhibited higher plasma ALT and AST levels, a marker of liver injury. In fact, there was a significant interaction between diet and PCB-126 for elevated plasma ALT (p= .0005) (Figure 2.2).

With regard to body weight (BW) and liver weight (LW), as anticipated both MCD groups demonstrated a decrease in the BW over the course of the 14-week study when compared to the CD-fed mice. The LW to BW (LW/BW) ratio was also determined and the MCD+ PCB-126 mice presented with the largest LW/BW when compared to all other groups (Figure 2.2).

2.3 PCB-126 Exposure in MCD fed mice Altered Hepatic Gene Expression of AhR Target Genes

Since activation of AhR is the major cellular mechanism by which dioxin-like PCBs exert their effects, the hepatic expression of genes related to PCB-126 initiated AhR activation were measured. As anticipated, the gene of expression of the AhR target gene cytochrome P450 1A2 (Cyp1a2*)* was upregulated in both groups exposed to PCB-126 (Figure 2.3). Another AhR target, flavin-containing monooxygenase 3 (Fmo3), was also measured and an interesting finding in this study was the hepatic gene expression was solely increased in the MCD+PCB-126 group. Since previous studies have shown that dioxin-like pollutants can increase hepatic Fmo3 expression, and this is correlated with an increased risk for CVD via TMAO synthesis, we also determined the hepatic and plasma TMAO

levels. Interestingly, hepatic gene expression of Fmo3 in addition to both hepatic and plasma TMAO levels were upregulated, and this result was only observed in the MCD+PCB-126 group. This finding is also important with regard to the gut-liver axis, as TMAO production is a result of the actions of both the gut microbiota and the liver.

2.3 PCB-126 Exposure Upregulated Markers of Peripheral Vascular Inflammation in MCD-Fed Mice

To determine whether a compromised liver could influence PCB-126 toxicity on other organ systems via systemic actions, we next examined the plasma profile of adhesion molecules and inflammatory cytokines (Figure 2.3). Interestingly, we observed an increase in markers of early endothelial cell injury in the MCD+PCB-126 group, as evidenced by increased levels of intercellular adhesion molecule 1 (Icam-1), platelet endothelial cell adhesion molecule (Pecam-1), E-selectin, P-selectin, thrombomodulin, and matrix metallopeptidase 9 (proMMP-9), with a significant interaction between diet and PCB-126 for Icam-1 ($p = .002$). With regards to peripheral vascular inflammation, similar to the results observed with markers of endothelial cell dysfunction, we also saw a significant increase in the systemic levels of inflammatory cytokines, Tnf-α and Mcp-1 in the MCD + PCB126 group. In fact, there was a significant interaction between diet and PCB-126 for both plasma Tnf-α and Mcp-1 ($p < .0001$).

Discussion

Since PCBs are persistent in the environment even though they were banned many years ago, studying the disease outcomes that are a direct result of and associated with the exposure to these chemicals is still necessary. It is well established that PCB-126 associated effects are driven by its activation of the AhR causing a cascade of events that ultimately leads to increased inflammation, disruption of the cellular redox status, liver injury, and other diseases [89-91]. Previous research in our lab showed that in the presence of a compromised liver, PCB toxicity was exacerbated by disrupting the energy homeostasis in NAFLD mice [19]. To further elicit how a compromised liver can specifically alter PCB-126 toxicity and influence cardio-metabolic disease outcomes, we examined the effects that PCB-126 exerted on the liver and peripheral vasculature.

Although PCB-126 alone was shown to induce ectopic fat accumulation in this study, PCB-126 in the presence of a compromised liver was the condition that contributed to the most pronounced hepatic and peripheral inflammation. The MCD+PCB-126 group exhibited worsened steatohepatitis as shown by hepatic H&E staining and increased gene expression of the inflammatory and fibrotic markers Mcp-1, Tnf-α, PAI-1, and Timp-1. This was also in conjunction with an increased LW/BW ratio and an increase in plasma ALT and AST, markers of toxicity and liver injury respectively. These findings suggest that in the presence of a compromised liver, PCB-126 induced hepatic toxicity is worsened.

In this study we also observed upregulated levels of the hepatic Fmo3, a downstream target of the AhR, in addition to increased levels of hepatic and plasma TMAO in MCD-fed mice exposed to PBC-126. Interestingly, TMAO is derived from the actions of both the gut-microbiota and the liver. The consumption of foods that is high in dietary choline and carnitine rich sources provides precursors that can be metabolized by the gut microbiota to trimethylamine (TMA). Next, hepatic FMO3 oxidizes TMA, forming TMAO. Interestingly, it has recently been shown in our lab that this pathway can be impacted by environmental factors, like dioxin-like PCBs as Petriello et al. showed that PCB-126 could possibly be a risk factor for CVDs because of its ability to upregulate Fmo3 [86]. The evidence linking dioxin-like PCBs, TMAO, and CVD risk is compelling with clinical studies showing that exposure to dioxin-like pollutants may contribute to elevated levels of serum TMAO in addition to linking this small organic compound and CVD [37, 92, 93]. However, the mechanisms relating TMAO to CVD risk is still unclear, with others reporting conflicting findings showing that increased TMAO levels can slow aortic lesion formation [94].

The findings in this present study raises two important questions. Firstly, if TMAO is derived from dietary choline and carnitine sources, how is it possible that we observed increases in the MCD+PCB-126 group when these mice were fed a diet absent of choline? A reasonable explanation is that the mice are using non-choline sources to form TMAO, however further investigation may be warranted. Secondly, since we observed such drastic effects of PCB exposure in

the MCD-fed mice with Fmo3 and TMAO levels and remembering that the TMAO molecule is derived from activities of the gut and the liver, what role does the gut microbiota play in the exacerbation of PCB-126 induced toxicity in this model? Future studies would need to be conducted to tease out the role that the gut-microbiota plays in PCB-126 induced toxicity in mice with liver injury.

Another interesting finding in this study was that the concomitant MCD+PCB-126 group exhibited a significant increase in both circulating inflammatory cytokines such as Tnf-α and Mcp-1 as well as early markers of peripheral vascular inflammation such as Icam-1, Pecam-1, E-selectin and thrombomodulin. The increase in plasma inflammatory makers supports the increase in hepatic inflammation reported above, showing that PCB-126 toxicity is worsening both hepatic and systemic inflammation. With regards to the upregulated markers vascular inflammation, we previously showed that PCB-126 can induce endothelial cell dysfunction via a similar mechanism in vitro, thus this finding was important as it confirms a similar phenotype in vivo [95].

Altogether, the findings in this study displayed that in the presence of a compromised liver PCB-126 toxicity is exacerbated, both hepatically and systemically. This study also provided a link between dioxin-like PCBs, the gut-microbiota, and the liver, implicating the gut-liver axis and associated circulating metabolites like TMAO in CVD risk. This is especially important for individuals that have pre-existing liver conditions and are subsequently exposed to environmental pollutants, as they may have an increased risk for the development of other associated inflammatory diseases like CVD.

Figure 2.1 Experimental design.

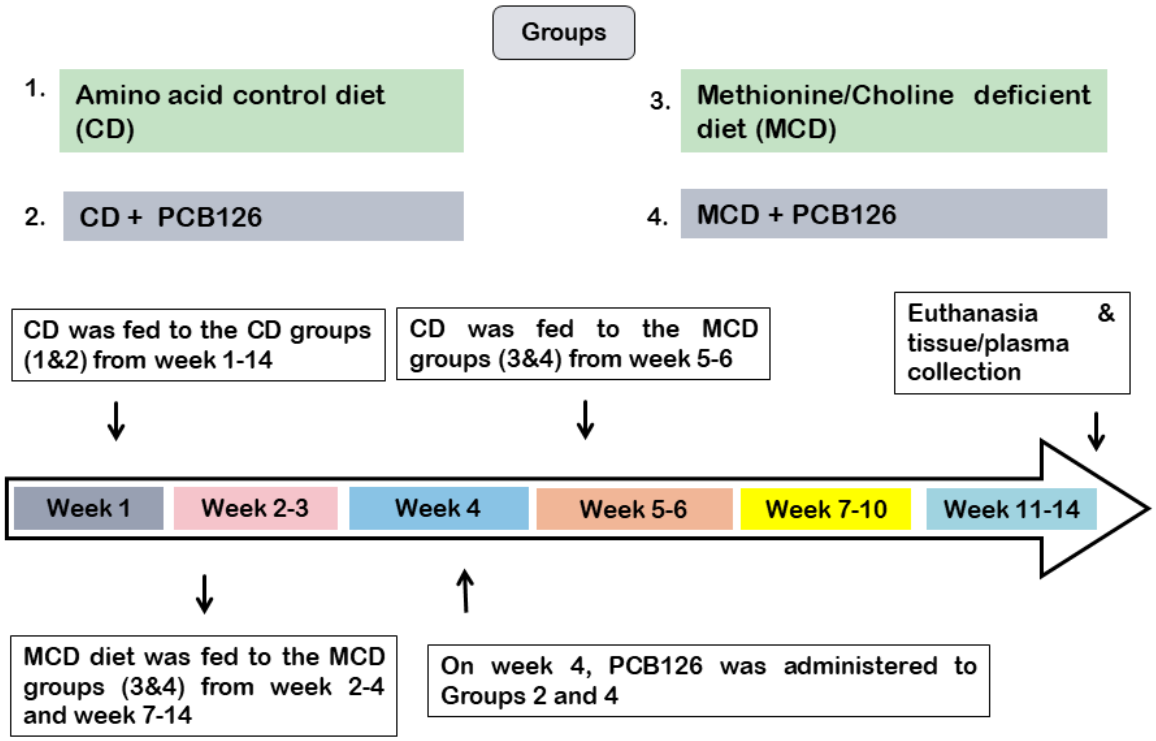

Figure 2.1 Experimental design. Mice were divided into 4 study groups (n=10) based on diet type (CD or MCD) and PCB126 exposure. The timeline for diet separation and PCB exposure regimen are also outlined in the figure. Figure adapted from *Wahlang et al.* Toxicol Sci, 2017. 160(2): p. 256-267.

Figure 2.2. Effects of PCB126 exposure on steatosis and BW.

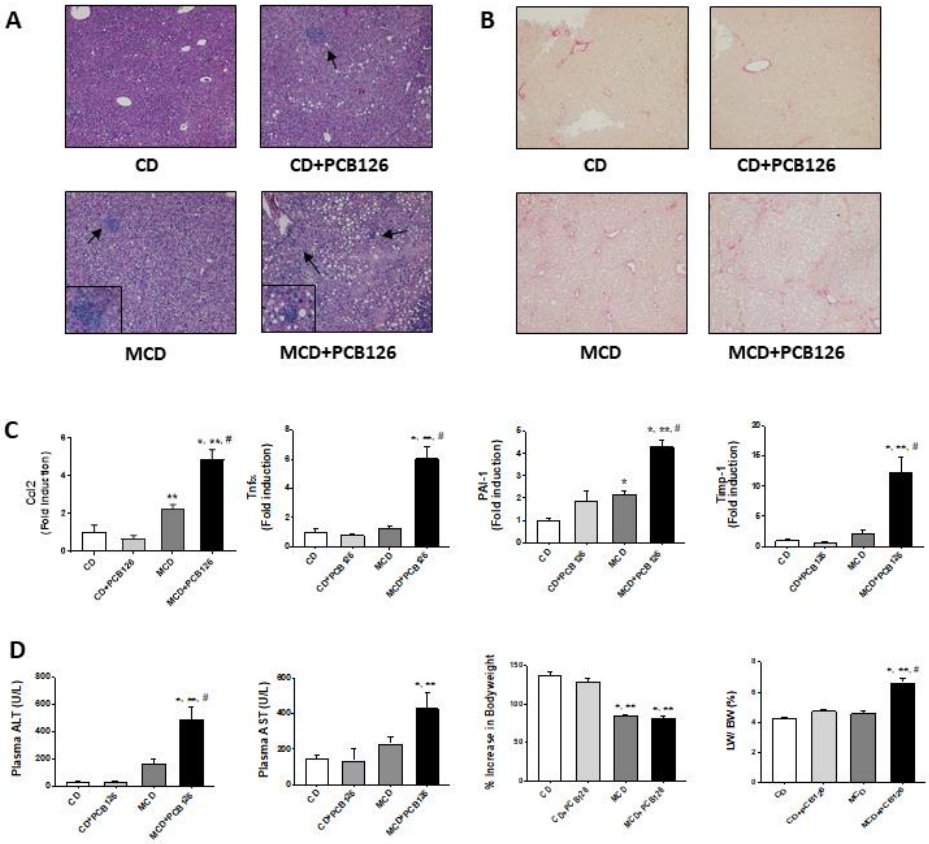

Figure 2.2. Effects of PCB126 exposure on steatosis and BW. A) H&E staining of hepatic sections established the occurrence of hepatocellular hypertrophy and steatosis in the MCD-fed groups. Each illustration is representative per treatment group B, Picrosirius red staining of hepatic sections indicated presence of fibrosis in the MCD groups. C, Hepatic mRNA expression for Ccl2/Mcp-1, Tnf-α, PAI-1 and Timp-1 were assessed. D, Plasma ALT and AST levels were measured using the Piccolo Xpress Chemistry Analyzer. Increase in BW with time for C57BL/6 (n=10) taken weekly from week 1-14. The % increase in BW gain with time was calculated and the BW at week 1 was taken as 100%. Livers were weighed at euthanasia and the liver to bodyweight ratio was calculated. Values are mean ±SEM, *p < .05 versus CD-fed mice, **p < .05 versus CD-fed mice exposed to PCB126, #p < .05 versus MCD diet-fed mice, ##p < .05 versus MCD-fed mice exposed to PCB126. Figure adapted from *Wahlang et al.* Toxicol Sci, 2017. 160(2): p. 256-267.

Figure 2.3. Effects of PCB126 on AhR target gene expression and TMAO levels.

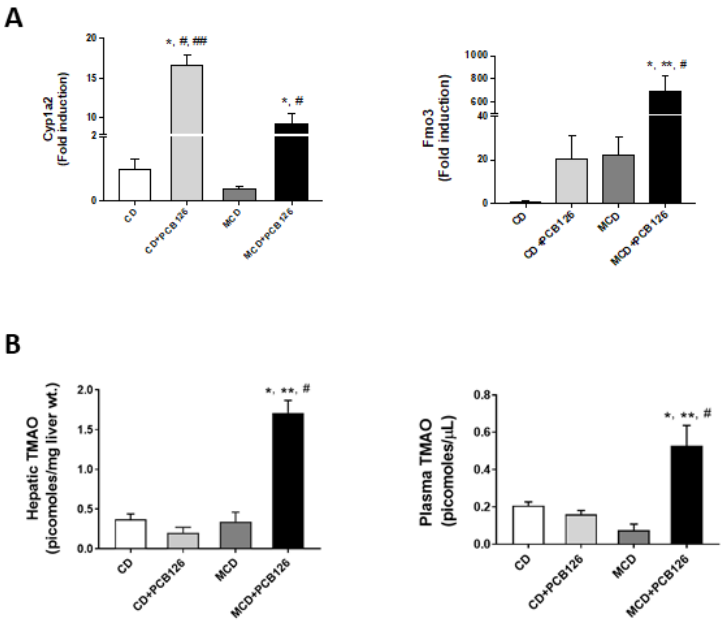

Figure 2.3. Effects of PCB126 on AhR target gene expression and TMAO levels. A, Hepatic mRNA expression for AhR target genes Cyp1a2 and Fmo3 were measured. B, TMAO was extracted from liver tissue and plasma and was measured using an ion trap triple quadrupole mass spectrometer. Figure adapted from *Wahlang et al.* Toxicol Sci, 2017. 160(2): p. 256-267.

Figure 2.4. PCB126 exposure increased circulating cytokine levels and markers of early vascular injury.

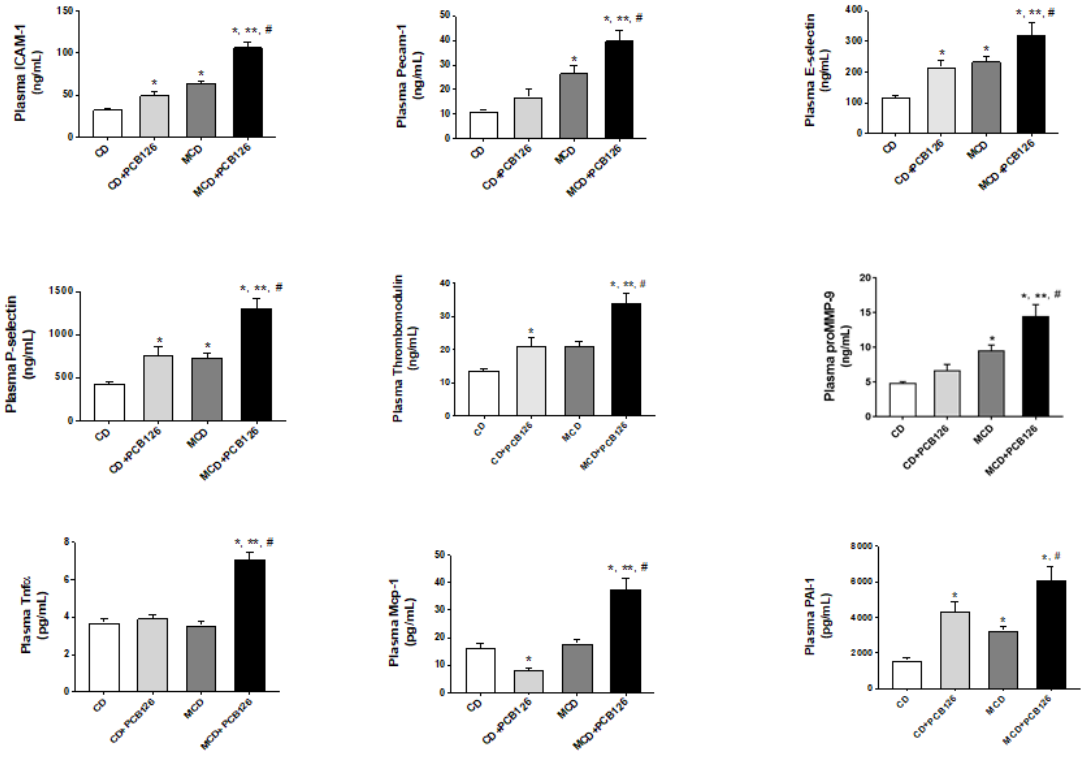

Figure 2.4. PCB126 exposure increased circulating cytokine levels and markers of early vascular injury. Plasma levels of Icam-1, Pecam-1, P-Selectin, E-selectin, thrombomodulin, proMMP9, Tnf-α, Mcp-1 and PAI-1 were measured using the MAGPIX system. Values are mean ± SEM, *p < .05 versus CD-fed mice, **p < .05 versus CD-fed mice exposed to PCB126, #p < .05 versus MCD diet-fed mice, ##p < .05 versus MCD-fed mice exposed to PCB126. Figure adapted from *Wahlang et al.* Toxicol Sci, 2017. 160(2): p. 256-267.

Chapter 3 Specific Aim 2: Test the hypothesis that the polyphenol-rich green tea extract (GTE) can protect against diet-induced liver injury in wild type C57BL/6 mice

Summary

SCOPE: Nonalcoholic fatty liver disease (NAFLD) can impact gut microbiota health and vice versa. Our previous worked showed that PCB-126 toxicity was worsened in mice with pre-existing liver injury, with implications that the gut-microbiota can possibly play a role in dioxin-like pollutant associated CVD risk [18]. A way to combat chronic inflammatory diseases is through nutritional modulation. Green tea extract (GTE) protects against NAFLD in multiple preclinical models, but its therapeutic effects are influenced by its bioavailability and no work in the more severe methionine-choline deficient (MCD) diet model has been completed. In addition, the interactions between MCD diet and GTE is not certain. Herein, we investigated whether GTE can protect against MCD-induced hepatic toxicity and the development of NAFLD.

METHODS AND RESULTS: In this 8 week study, mice were fed an amino acid control diet or a diet that induces liver injury in the absence or presence of GTE resulting in four experimental groups: control diet (CD), CD+ GTE, MCD, and MCD+ GTE. Histological parameters, inflammatory markers, GTE metabolism, and gut microbiota diversity were examined. Results indicated that MCD mice exhibited severe liver injury and gut dysbiosis and unexpectedly GTE had no

protective effects. Interestingly, MCD mice displayed differential epigallocatechin-3-gallate (EGCG) metabolism at the hepatic and gut microbiota level which may alter polyphenol bioavailability and therapeutic potential.

CONCLUSIONS: These results provide insight into how a dysfunctional liver and gut dysbiosis can alter polyphenol metabolism, possibly reducing its therapeutic efficiency. This is important for individuals with NAFLD that utilize beneficial polyphenols as a means of disease intervention.

Introduction

The liver is the primary site for endobiotic and xenobiotic metabolism, hence its proper function is crucial for the body's response to innate and extrinsic insults. Nonalcoholic fatty liver disease (NAFLD) is a major public health problem as its prevalence has steadily increased with an estimated 25% of the world's population affected by this disease [7, 8]. NAFLD is the hepatic manifestation of metabolic syndrome and represents a spectrum of progressive diseases that ranges in severity from steatosis (fat accumulation) to steatohepatitis (steatosis and inflammation), to cirrhosis (advanced fibrosis), and eventually hepatocellular carcinoma or liver failure [7]. NAFLD pathophysiology is multifaceted and the causative mechanisms remain unclear, yet, a two or even multiple "hit" hypothesis has been proposed. This begins with an imbalance of the synthesis, influx, oxidation and export of hepatic lipids followed by a second "hit" initiated by oxidative stress, or gut-derived components that induces inflammation and/or fibrosis [14, 15]. In addition, the liver's unique and significant blood supply via the portal and hepatic veins allows for anatomical and functional interactions with other organs and vice versa including the kidneys, the heart, and the gastrointestinal tract [96, 97]. This cross talk between organs is becoming a focus in disease development and progression with a new focus on the interactions between the gut and the liver, named the "gut-liver axis" being studied more in recent literature [97].

The gut microbiota is the diverse microbe population that resides in the gastrointestinal tract. It plays a major role in overall host health by aiding in

digestion, contributing to metabolism of dietary and host-derived molecules, combating other microorganism, and acting as a first line of defense to the external environment [98]. Additionally, the gut microbiota's location makes it susceptible to dietary manipulation and current studies seek to identify techniques to alter disease risk using nutritional therapeutics targeting the gut [29, 30]. An imbalance of the intestinal flora, known as gut dysbiosis, is associated with disease development such as NAFLD [31]. Interestingly, the gut microbiota and the liver have been shown to participate in a partnership, known as the gut-liver axis, and has been associated with the development, progression, and exacerbation NAFLD [22].

One way to combat the deleterious effects of fatty liver disease is by increasing consumption of beverages and foods that contain beneficial bioactive nutrients, dietary polyphenols. Tea is the 2nd most consumed beverage on the globe and in particular green tea and its major bioactive polyphenolic catechin epigallocatechin-3-gallate (EGCG) has been well studied as a therapeutic for NAFLD using *in vivo* models in recent years [59-61]. Although the mechanisms by which EGCG and other green tea polyphenols exert their protective effects are unclear, these compounds can decrease expression of hepatic transcription factors involved in downstream inflammatory responses [64] and increase expression of transcription factors involved in the activation of antioxidant response [63], resulting in anti-inflammatory and anti-oxidant properties respectively in rodent models of fatty liver disease. Still, these properties of

dietary polyphenols are subject to their bioavailability which is directly dependent on the activity of the liver.

Since modifications in diet and nutrition, such as increased consumption of green tea, has historically been used as a method to combat disease and is dependent on a healthy liver, it is important to investigate the mechanisms by which tea polyphenols can protect against severe liver disease. Hence the objective of this present study was to investigate if GTE could protect against the hepatic toxicity associated with MCD-induced NAFLD.

Experimental design and methods

Animals, diet, and experimental design

The animal protocol was approved by the University of Kentucky Institutional Animal Care and Use Committee. Animals were housed in a temperature- and-light controlled room on a 12 hour light/dark cycle with food and water *ad libitum*. Forty male C57BL/6 mice were purchased from Taconic (Hudson, NY, USA) and evenly divided into four study groups. Mice were fed either a purified amino acid control diet (CD; TD.130936; Envigo) or methionine-choline deficient diet (MCD; TD.90262; Envigo) with or without supplementation of green tea extract (GTE; Sunphenon 30S-O,Taiyo, Minneapolis, MN, USA) at 1% (w/w) in diet. On Week 1 mice were fed either CD or CD+GTE and beginning week 2 appropriate groups were fed MCD diet to induce liver injury, yielding the following 4 experimental groups: CD, CD+GTE, MCD, and MCD+GTE. All mice fed MCD diets were reverted back to their respective control diets for one week

(week 5) of this total 8 week study (Figure 3.1). This measure was taken to avoid excessive weight lost and subsequent non-compliance with the IACUC protocol. Bodyweight was measured weekly. At the completion of week 8, animals were humanely euthanized and tissues were harvested for mRNA or protein and stored at - 80 °C.

Dosage Information

GTE was supplemented in the animal diets at 1% wt/wt. The in vivo dose was chosen based on previous studies [99]. The amount of GTE per body weight in this study is comparable to approximately 4 cups of tea (~200 mL/cup) consumed per day in humans [100]. This dose is achievable through regular diets.

Histological examination

Hepatic tissues were fixed in 10% neutral buffered formalin and embedded in paraffin for histological assessment. Tissue sections were stained with hematoxylin and eosin (H&E) and examined by light microscopy. Images were captured using a high resolution digital scanner at 10x magnification.

Metabolic profile assessment and urine collection

At week 8 of the study, three mice from each group were randomly selected (n=3) and placed into metabolic cages individually (Techniplast, Exton, PA, USA). Urine samples were collected in the 24-hrs period and stored at -80°C

until analyzed. Three samples from each group were pooled proportionated to the urine volume of each mice. The pooled samples (~150 µL) were extracted using methanol. After centrifugation, the supernatant was dried under nitrogen flow. The residue was resolved in a mixed solution of acetonitrile: water (9:1, v/v), and 5 µL of sample was injected for LC-MS analysis. An ultra-high performance liquid chromatography Q-Exactive mass spectrometer (Thermo Fisher Scientific, San Jose, CA) was used for sample detection. Chromatographic separation was performed on a reversed phase Kinetex C18 column (2.6 mm × 100 mm, 2.1 µm, Phenomenex, USA). Mobile phases were composed of acetonitrile (A) and water (B), both containing 0.1% formic acid. The column temperature was maintained at 40°C, and the flow rate was set to 0.4 ml/min. Mass spectrometric detection was performed by electrospray ionization in positive ionization mode with source voltage maintained at 4.3 kV. The capillary temperature, sheath gas flow and auxiliary gas flow were set at 330°C, 35 arb and 12 arb, respectively. Full-scan MS spectra (mass range m/z 75 to 1000) were acquired with resolution R = 70,000 and AGC target 1e6. MS/MS fragmentation was performed using high-energy C-trap dissociation with resolution R = 35,000 and AGC target 2e5. The stepped normalized collisional energy scheme was set at 30, 40, and 50. Raw data files acquired in full scan-ddMS2 mode were imported into Compound Discoverer™ software (v. 2.1; Thermo Fisher Scientific) to identify EGCG, ECG, EGC, and EC metabolites respectively. The software detects chromatographic peaks, and the mass of the corresponding compound is compared with a list of generated theoretical metabolites. Potential metabolites were proposed based on

exact mass, MS2 fragmentation, isotopic pattern and retention time with respect to the parent compound.

Blood collection and plasma protein quantification

Post euthanasia blood samples were collected, mixed briefly with EDTA, and centrifuged at 2000 g for 15 minutes at 4 °C to isolate plasma. Plasma samples were frozen in liquid nitrogen and stored at - 80 °C until further processing. Plasma alanine transaminase (ALT) and aspartate transaminase (AST) levels were measured using the Piccolo Xpress Chemistry Analyzer using Lipid Panel Plus reagent disks (CLIAwaived Inc., San Diego, CA, USA).

RNA extraction and quantitative real-time PCR

Intestinal and liver samples were homogenized and total mRNA was isolated with TRIzol reagent (Invitrogen, Carlsbad, CA, USA). mRNA purity and quantity were determined using the NanoDrop 2000 spectrophotometer (Thermo Fisher Scientific Inc., Waltham, MA, USA) using the NanoDrop 2000 version 1.6.198 and cDNA was synthesized from total RNA using the QuantiTect Reverse Transcription Kit (Qiagen, Valencia, CA, USA). PCR was performed using the Taqman Fast Advanced Master Mix (Thermo Fisher Scientific Inc.) on the CFX96 Touch Real-Time PCR Detection System (Bio-Rad, Hercules, CA, USA). All primers were acquired from Taqman Gene Expression Assays (Thermo Fisher Scientific Inc.). The mRNA levels were normalized relative to the quantity

of Actb for intestinal samples or Rn18s for liver samples and levels of gene expression were calculated using the $2^{-\Delta\Delta Ct}$ method.[88]

Cecum DNA extraction and 16S rRNA sequencing for bacterial taxonomy

At the conclusion of the study, cecum samples were sent to Argonne National Laboratory. DNA extraction and 16S sequencing was performed by the Environmental Sample Preparation and Sequencing Facility (ESPSF) and analyzed by the Quantitative Insights into Microbial Ecology (QIIME) program. DNA extraction was conducted using the PowerSoil 96-well DNA Isolation Kit (MoBio, Carlsbad, CA, USA) according to the manufacturer's protocol with the addition of a 65°C heating step after solution C1 addition. The protocol used for the production of the PCR amplicon library, amplicon quantification and sequencing, and operation taxonomic units (OTUs) selection and filtration is outlined in Petriello, M.C. and Hoffman, J.B., et al.[28]

Statistical Analysis

A University of Kentucky biostatistician was consulted for data analysis. For cecum bacterial phyla tables, for each type of bacteria, relative abundance means, and standard errors were calculated for each of the four groups. Next, a full factorial two-way beta regression model was fit using the "betareg" package in R, analyzing differences in relative bacterial abundance between CD and MCD diets and in the presence or absence of green tea extract supplements. Reported *p*-values come from a likelihood ratio test of the overall model fit. All

analyses were completed in R, version 3.4.4 (R Foundation for Statistical Computing; Vienna, Austria). For all other data, statistical analyses were conducted and graphs were plotted using GraphPad Prism version 7.02 for Windows (GraphPad Software Inc., La Jolla, CA, USA). Data are expressed as mean ± SEM. Multiple group data was compared using Two Way ANOVA (column factor: diet row factor: GTE) followed by the Tukey's post-hoc test for multiple comparisons. For all data presented in this chapter, p-values < 0.05 was considered statistically significant.

Results

3.1 Experimental design

The experimental design for this study is presented in Figure 3.1.

3.2 GTE does not protect against MCD-induced hepatic steatosis and inflammation

In an effort to examine the effect that GTE supplementation had on MCD-induced liver injury, hepatic steatosis was assessed histologically and inflammation assessed via histology, hepatic gene expression, and plasma cytokine measurements. MCD diet feeding resulted in severe hepatic steatosis and inflammation, consistent with previous studies. Additionally, H&E staining revealed an increase in ectopic fat deposition in the hepatocytes of the MCD groups in addition to the presence of inflammatory foci, an indication of steatohepatitis (Figure 3.2). This was further proven with a significant increase in

macrovesicular fat content in all MCD fed mice as determined by a liver pathologist (Figure 3.2). We also observed a decrease in the liver weight (LW) of mice fed MCD diet when compared to both control groups (Figure 3.2).

With regards to inflammation, the hepatic mRNA expression was determined by qPCR analysis. The gene expression of inflammatory markers including Tumor necrosis factor alpha (Tnf-α), C-C motif chemokine ligand 2 (Ccl2) also called Monocyte chemoattractant protein-1 (Mcp1), and Plasminogen activator inhibitor-1 (Pai-1) were all increased in mice with liver injury, and GTE supplementation did not have any protective effects (Figure 3.2). Furthermore, liver injury was further confirmed by significantly increased amounts of ALT in the plasma of MCD fed mice compared to both CD fed groups was observed in addition to an increase in plasma AST in MCD groups when compared to the mice fed CD only (Figure 3.2). Taken altogether, this data ascertains that MCD diet feeding contributed to liver injury by increased hepatic fat accumulation and inflammation and GTE supplementation had no significant effects on any outcomes associated with the development and progression of hepatic steatosis or inflammation.

3.3 Liver injury alters hepatic and gut microbiota catalyzed green tea metabolite profile

Since we did not see any GTE protection from MCD-induced liver injury, we then sought to understand whether there were alterations in GTE metabolism due to this severe disease state. We examined the GTE urine metabolite profile

at the end of the study. At week 8, mice from each group (n=3) were placed into solo urine collection cages for 24 hours and the GTE metabolite profile was measured via LC-MS. Interestingly, mice with a dysfunctional liver exhibited an increase in the urine excretion of parent compounds EGCG and ECG while on the contrary, these mice displayed a decrease in the corresponding metabolites EGC and EC respectively (Figure 3.3). Furthermore, mice with liver injury demonstrated an increase in overall glucuronides and sulfation conjugation GTE metabolites and a decrease in the overall methylation (Figure 3.3 and Table 3.1). In addition, a significant decrease in the gut microbiota catalyzed ring fission metabolites was seen in MCD diet fed mice, with 5-dihydroxyphenyl valeric acid and its conjugates being the major metabolites (Table 3.2).

3.4 Liver injury modifies expression of hepatic, not intestinal, phase 2 metabolizing enzymes and transporters

To further delineate the mechanisms associated with the GTE metabolism changes that were observed in mice with liver injury, we next examined the gene expression of conjugation enzymes and membrane transporters in the intestines and the liver. In the intestines, there were no changes in the gene expression of catechol-O-methyltransferase (Comt), UDP-glucuronosyltransferase 1-1 (Ugt1a1), or sulfotransferase family 1b member 1 (Sult1b1) which translate to proteins that play major roles in metabolism via transfer of a methyl group, glucuronic acid group, or a sulfate group respectively (Figure 3.4). In addition, there was no observed changes in the intestinal gene expression of the

transporter ATP-binding cassette sub-family C member 2/ multidrug resistance-associated protein 2 (Abcc2/Mrp2). Similar to the intestinal gene expression, hepatic Comt and Ugt1a1 were unchanged. However, hepatic gene expression of sulfotransferase family 1a member 1 (Sult1a1) and the transporter Abcc2/Mrp2 was significantly increased in the MCD+GTE mice when compared to all other groups. We also observed increased levels of the transporter ATP-binding cassette sub-family C member 2/ multidrug resistance-associated protein 1 (Abcc1/Mrp1) gene in both MCD groups (Figure 3.4).

3.5 MCD-induced liver injury alters the bacterial phyla profile and the FB ratio

Recent studies have begun to delineate the mechanisms by which the gut-liver axis can contribute to disease pathology and influence host health. To further understand the role that the gut-liver axis can plays in NAFLD development and progression as well as the effects it can exert on nutrient metabolism, 16S rRNA sequencing was conducted at the completion of the study to quantify bacterial populations. Cecal samples were utilized as the cecum serves as the principal site of bacterial metabolism and fermentation, in addition to having the greatest abundance of microbiota. We observed a major shift in the microbiota profile of MCD diet fed mice (Table 3.3).The MCD groups exhibited alterations in the taxonomic composition of the cecal microbiota at the phylum level at sacrifice (Figure 3.5). When compared to all other groups, the MCD+GTE group exhibited an increase the alpha diversity (Shannon diversity index), a measure of gut microbiota diversity within a sample and measures the number of

different microbes (richness) and the distribution of different microbes (evenness) (Figure 3.5). With regard to the *Firmicutes/Bacteroidetes* (FB) ratio the MCD group's ratio was increased when compared to both control groups and GTE supplementation decreased this effect, although this was not statistically significant (p=0.08) (Figure 3.5).

3.6 MCD fed mice exhibits gut dysbiosis via alterations in the cecal bacterial profile

Interestingly, at the phyla level, MCD-induced liver injury significantly increased the abundance of the *Tenericutes* bacterial phyla (Figure 3.6). More specifically at the corresponding order level, the bacteria RF39 was increased in MCD fed mice. Moreover, the phyla *Verrucomicrobia* was significantly increased in both MCD diet fed groups and GTE supplemented groups, and this was accompanied by an increase in the corresponding genus *Akkermansia* (Figure 3.6). We also observed a decrease in the abundance of the bacterial phyla *Bacteroidetes* and its parallel genus *Parabacteroides* in the MCD group when compared to both control groups (Figure 3.6). These findings showed that MCD diet can alter cecal bacterial profiles, causing gut dysbiosis.

Discussion

NAFLD is still a major public health concern, with nearly one-fourth of the world's inhabitants suffering from this disease. The liver is a vital organ in the body and proper metabolism and overall host health is dependent on it being in a

healthy state. One factor that can contribute to the development and/or progression of NAFLD is the secretion of gut-derived components that act on the liver as a result of gut dysbiosis [22]. A way to combat the deleterious effects seen with NAFLD is through changes in diet and lifestyle with recent clinical guidelines suggesting an increase consumption of foods and beverages rich in naturally occurring antioxidant components as a way to prevent and treat NAFLD [101].

Green tea has historically been used to prevent or attenuate multiple chronic inflammatory disease including NAFLD, but it's important to remember that its therapeutic capabilities may be dependent on its metabolism and bioavailability [62, 102]. Hence, the primary aim of this study was to investigate if GTE could protect against the hepatic toxicity associated with MCD-induced NAFLD.

Consistent with our previous studies and the work of others, we saw that MCD diet feeding induced steatohepatitis by increasing hepatic fat accumulation and inflammation [18, 19, 103]. Steatosis was evidenced by H&E staining and an increase in the macrovesicular fat content. There was also a significant decrease in the LW of MCD groups versus both CD groups. This was accompanied by an increase in inflammation as seen by increased gene expression of the hepatic inflammatory markers TNF-α, Ccl2, and Pai-1 in addition to a significant increase in plasma ALT in MCD diet fed mice when compared to CD groups. In addition, we observed an increase in the plasma levels of AST in MCD mice when compared to the CD only fed group was also observed. These result were

anticipated as the MCD diet is a highly utilized and robust rodent model of NAFLD, with continual feeding causing fat accumulation and inflammation and/or fibrosis, leading to the end stage of fatty liver disease known as NASH [104]. However what was unexpected was the finding that GTE supplementation did not protect against MCD-induced hepatic steatosis or inflammation.

Nutritional intervention has been historically used as a natural and feasible method to combat chronic, inflammatory disease. However, because most endogenous and exogenous components are metabolized by the intestines and in the liver, it is important to investigate how a dysfunctional liver can alter the metabolism of beneficial dietary components that are intended to prevent or reduce disease risk. Since we observed hepatic injury, we then sought to understand how this phenotype could influence the metabolism, and possibly the lack of protection, of the GTE.

In this study, MCD fed mice exhibited a significant increase in the urine excretion of both the parent compounds EGCG and ECG while their respective metabolites EGC and EC were decreased. Others have reported a similar result with Chen et al. reporting that obese rats had higher excretion of EGCG and ECG and the absence of EGC and EC in the feces after oral administration of tea polyphenols [105]. The increased EGCG and ECG excretion may be dependent on multiple mechanisms, including the efflux by transporters such as Abcc2. Abcc2 is a major efflux transporter that resides on the canalicular membrane of hepatocytes and is responsible for substrate transport, including elimination of conjugated substances [106, 107]. Furthermore, it has been reported that during

the progression of human NAFLD Abcc1 and Abcc2 expression is increased [108]. Interestingly, Hong et al. concluded from studies in a canine kidney cell line that EGCG and its metabolites can be substrates for Abcc2 [109]. It is reasonable to suggest that this observation is related to the increase of EGCG in the urine of MCD fed mice. The decrease in the presence of EGC and EC may be because of its metabolism into low molecular-weight phenolic acids, as seen in other studies in rats [105].

An interesting finding in this study related to GTE metabolism was the observed increase in GTE sulfation metabolites. To further explain this increase, the hepatic gene expression of the conjugation enzyme Sult1a1 was measured via qPCR. Sult1a1 is a major drug-metabolizing enzyme that catalyzes the sulfate conjugation to many endogenous and exogenous compounds. We observed a significant increase in the gene expression of Sult1a1 solely in the MCD+GTE group which could support the increase we saw in sulfate conjugated GTE metabolites that was seen in MCD diet fed mice. In this study, we also observed an increase in glucuronidation GTE metabolites in MCD diet fed mice. We followed up with this finding by examining the gene expression of Ugt1a1 in the intestines and the liver. Surprisingly, the expression of Ugt1a1 was unchanged in both the intestines and the liver. Further analysis looking into other glucuronidation enzymes will need to be conducted to determine why this increase was observed.

Another major metabolic change that was seen was the significant decrease in GTE methylation metabolites in the urine. Comt is one of several

enzymes that is responsible for the degradation of catecholamines such as epinephrine and dopamine and any other compounds that have a catechol entity. Many drugs have been developed to target this enzyme. The presence of a catechol-like structure, like that seen in EGCG and ECG as well as their resulting metabolites, makes these compounds susceptible to methyl addition by both rodent and human Comt [110, 111].

We observed an increase in methylation GTE metabolites in the urine of mice with liver injury, however there was no change in the hepatic gene expression of Comt in any of the experimental groups. Interestingly, the Comt enzyme activity is dependent on the donation of a methyl group from S-adenosyl methionine (SAM) and we (unpublished data) have shown that in MCD diet fed mice, the SAM cofactor was depleted. This is plausible, as the MCD diet lacks the essential amino acid methionine, which is involved in SAM synthesis [50-52]. In fact, other models of NAFLD, including high fat diet feeding, also shows a significant reduction in the SAM co-factor [112]. We believe this explains why we observed a decrease in methylation GTE metabolites without an expressional change in the intestinal or hepatic gene expression of Comt.

Furthermore, liver injury in mice fed MCD diet also had a significant decrease in the gut microbiota catalyzed ring fission metabolites. Specifically, the metabolite 5-dihydroxyphenyl valeric acid and its conjugates were the major metabolites, as seen by an increase in the peak area. Meng et al. reported that in healthy humans and rodents administered green tea or ECGC, the ring fission metabolites were identified by LC-MS at significant amounts in the plasma and in

the urine, implicating the intestinal microbiota in green tea and EGCG metabolism [113]. However, research investigating the gut microbiota catalyzed metabolism of GTE and its major polyphenolic constituents is still lacking.

After confirming liver injury in mice fed MCD diet and that GTE displayed no protection against hepatic injury with a major shift in the hepatic and gut microbiota catalyzed metabolic profile, we then sought to understand the role of the gut microbiota in the observed metabolic changes and overall host health. Remarkably, alterations in the cecal gut microbiota profile was seen in mice fed the MCD diet. In comparison to all other groups, the alpha diversity was increased in the MCD+GTE mice. In particular, we observed no changed in the *Firmicutes* phylum in both MCD groups when compared to the CD only fed group. With regard to the *Bacteroidetes* phylum, we observed a decrease in mice fed the MCD diet only when compared to the CD only fed group. This finding was also seen in human studies of patients with NAFLD with Mouzaki et al. reporting a decrease in fecal *Bacteroidetes* [20]. However, when examining these two phyla, the ratio of *Firmicutes* to *Bacteroidetes* (FB ratio) may be a more important parameter to assess as an increase in the FB ratio has been positively correlated with NAFLD in addition to an increased susceptibility to oxidative stress and inflammation [114]. In this study, we observed a significant increase in this ratio in mice with liver injury and GTE supplementation seemed to attenuate these effects ($p=0.08$). This suggests that MCD feeding exerts some negative effects on the intestinal gut flora and that GTE exerts some protective effects, although the finding in this study was statistically insignificant.

Additionally, MCD feeding significantly increased the *Tenericutes* phylum as well the corresponding order RF39. In recent literature, Rau et al. reported a significant decrease in the fecal abundance of *Tenericutes* in human patients with NASH while Ye, Li, and Wu et al. reported that mice fed MCD diet showed a significant increase in *Tenericutes as* compared to that of CD mice [115, 116]. However, the *Tenericutes* phyla has been poorly studied and there is a sufficient lack of evidence and information investigating this phyla in metabolic syndrome and fatty liver disease.

In conclusion, our current study demonstrates that GTE cannot protect against severe liver injury as seen in this MCD mouse model. However, diet-induced liver injury in conjunction with guy dysbiosis can alter the metabolite profile of GTE, possibly impacting the protective properties of GTE. The findings of this study has translational implications as proposed interventions for individuals with liver disease typically includes changes in diet and lifestyle, particularly by encouragement to increase consumption of nutrient rich and lower fat foods. Future studies are needed to determine the causative mechanisms by which the gut-liver axis can contribute to altered nutrient metabolism and how this can influence overall health in humans.

Acknowledgments

J.B and P.D made equal contribution to the study. M.C.P., J.B.H, and C.W. assisted for in vivo models. E.L assessed H&E stained hepatic sections. A.J.M. contributed to LC-MS analysis. All the authors wrote and/or revised the manuscript. The authors would like to acknowledge Dr. Travis Sexton (UK Saha Cardiovascular Research Center), Dr. Wendy Katz (UK COBRE Research Core), the University of Louisville, and Greg Hawk and Dr. Arnold Stromberg for assisting with operation of the MAGPIX, metabolic cages, Piccolo Xpress chemistry analyzer, and assistance with statistical analysis respectively.

Funding Sources

This study was supported by the National Institute of Environmental Health Sciences [P42ES007380] and the National Institute of General Medical Sciences [P20GM103527] at the National Institutes of Health. The content is solely the responsibility of the authors and does not necessarily represent the official views of the National Institutes of Health.

Conflict of Interest

The authors have no competing or conflicts of interests to declare.

Table 3. 1.Summary of phase II GTE metabolites in mice urine.

Metabolites	m/z	Formula	Rt	LC-MS Peak Area	
	$[M-H]^-$		min	CD+GTE	MCD+GTE
EGCG	457.078	$C_{22}H_{18}O_{11}$	8.58	6.77E+05	1.28E+07
EGCG+methyl	471.093	$C_{23}H_{20}O_{11}$	9.17	ND	9.01E+05
EGCG+methyl	471.093	$C_{23}H_{20}O_{11}$	9.46	ND	9.01E+05
EGCG+Glu	633.110	$C_{28}H_{26}O_{17}$	8.90	ND	3.18E+06
EGCG+methyl+Glu	647.126	$C_{29}H_{28}O_{17}$	8.70	ND	4.16E+06
EGCG+diGlu-2H	807.164	$C_{34}H_{32}O_{23}$	9.93	1.10E+05	4.10E+05
EGCG+diGlu	809.142	$C_{34}H_{34}O_{23}$	8.37	8.90E+05	6.05E+06
EGCG+methyl+diGlu	823.158	$C_{35}H_{36}O_{23}$	9.21	2.72E+05	6.37E+05
ECG	441.082	$C_{22}H_{18}O_{10}$	9.67	2.80E+05	5.11E+06
ECG+methyl	455.098	$C_{23}H_{20}O_{10}$	8.36	8.78E+05	3.01E+05
ECG+SO3	521.040	$C_{22}H_{18}O_{13}S$	11.10	ND	1.29E+06
ECG+Glu	617.116	$C_{29}H_{28}O_{16}$	9.82	ND	3.78E+06
ECG+methyl+SO3	535.055	$C_{23}H_{20}O_{13}S$	11.43	ND	1.22E+06
EGC+methyl+Glu	645.146	$C_{30}H_{30}O_{16}$	10.20	ND	1.14E+06
ECG+diGlu	793.148	$C_{35}H_{36}O_{22}$	9.31	9.44E+05	9.07E+06
EGC	305.066	$C_{15}H_{14}O_7$	5.07	6.52E+06	1.39E+07
EGC+methyl	319.082	$C_{16}H_{16}O_7$	8.65	1.86E+06	3.23E+05
EGC+SO3	385.023	$C_{15}H_{14}O_{10}S$	5.97	1.13E+07	3.36E+07
EGC+SO3	385.023	$C_{15}H_{14}O_{10}S$	2.71	1.72E+07	7.58E+07
EGC+methyl+SO3	399.039	$C_{16}H_{16}O_{10}S$	8.23	2.10E+08	9.48E+07
EGC+Glu	481.099	$C_{21}H_{22}O_{13}$	5.50	1.20E+07	1.20E+07
EGC+Glu	481.099	$C_{21}H_{22}O_{13}$	2.56	6.95E+05	2.36E+07
EGC+methyl+Glu	495.114	$C_{22}H_{24}O_{13}$	7.54	4.01E+07	1.99E+07
EGC+diGlu	657.132	$C_{27}H_{30}O_{19}$	7.42	9.00E+05	1.22E+06
EC	289.072	$C_{15}H_{14}O_6$	8.25	1.30E+06	3.77E+06
EC+methyl	303.087	$C_{16}H_{16}O_6$	9.29	7.25E+05	1.17E+05
EC+SO3	369.028	$C_{15}H_{14}O_9S$	8.15	8.27E+07	1.14E+08
EC+methyl+SO3	383.044	$C_{16}H_{16}O_9S$	9.26	8.17E+06	2.70E+07
EC+methyl+SO3	383.044	$C_{16}H_{16}O_9S$	8.84	1.72E+06	2.08E+06
EC+methyl+SO3	383.044	$C_{16}H_{16}O_9S$	7.99	1.11E+06	1.11E+06
EC+Glu	465.103	$C_{21}H_{22}O_{12}$	6.73	1.12E+07	4.94E+07
EC+Glu	465.103	$C_{21}H_{22}O_{12}$	8.32	1.22E+06	1.81E+06
EC+Glu	465.103	$C_{21}H_{22}O_{12}$	7.76	1.71E+06	2.30E+06
EC+methyl+Glu	479.120	$C_{22}H_{24}O_{12}$	8.86	1.30E+06	9.71E+05
EC+methyl+Glu	479.120	$C_{22}H_{24}O_{12}$	8.37	2.65E+06	2.53E+06
EC+methyl+Glu	479.120	$C_{22}H_{24}O_{12}$	8.61	2.56E+06	4.31E+06

Table 3. 1. **Summary of phase II GTE metabolites in mice urine.** At week 8, mice from each group (n=3) were placed into solo metabolic cages and urine samples were collected over 24 hours. Pooled urine was extracted using methanol and analyzed by UHPLC/Q Exactive MS. Data was processed by CompoundDiscover and LC-MS peak area for each metabolite was calculated. J.B and P.D contributed equally to sample collection. P.D. analyzed data and made figure.

Table 3. 2. Gut microbiome catalyzed GTE metabolites in mice urine.

Metabolites	m/z	Formulae	Rt	LC Peak Area	
	$[M-H]^-$		min	CD	MCD
5-dihydroxyphenyl-γ-valerolactone+SO3	287.0231	$C_{11}H_{12}O_7S$	5.04	1.93E+07	1.93E+07
5-dihydroxyphenyl-γ-valerolactone+Glu	383.0984	$C_{17}H_{20}O_{10}$	6.68	1.11E+06	ND
5-trihydroxyphenyl-γ-valerolactone+SO3	303.0180	$C_{11}H_{12}O_8S$	2.20	1.72E+07	1.90E+06
5-trihydroxyphenyl-γ-valerolactone+Glu	399.0933	$C_{17}H_{20}O_{11}$	2.55	1.10E+06	ND
5-hydroxyphenyl valeric acid +SO3	273.0438	$C_{11}H_{14}O_6S$	9.71	ND	1.62E+07
5-hydroxyphenyl valeric acid +Glu	369.1191	$C_{17}H_{22}O_9$	9.81	ND	1.31E+06
5-dihydroxyphenyl valeric acid +SO3	289.0387	$C_{11}H_{14}O_7S$	8.10	7.11E+07	2.98E+07
5-dihydroxyphenyl valeric acid +SO3	289.0387	$C_{11}H_{14}O_7S$	9.29	5.30E+07	3.25E+06
5-dihydroxyphenyl valeric acid +Glu	385.1140	$C_{17}H_{22}O_{10}$	7.98	3.00E+06	7.01E+05
5-dihydroxyphenyl-4-hydroxyvaleric acid+SO3/5-trihydroxyphenyl valeric acid +SO3	305.0337	$C_{11}H_{14}O_8S$	7.12	3.99E+07	5.59E+05
5-dihydroxyphenyl-4-hydroxyvaleric acid+Glu/5-trihydroxyphenyl valeric acid +Glu	401.1089	$C_{17}H_{22}O_{11}$	7.85	5.13E+05	ND

Table 3. 2. Gut microbiome catalyzed GTE metabolites in mice urine. At week 8, mice from each group (n=3) were placed into solo metabolic cages and urine samples were collected over 24 hours. Pooled urine was extracted using methanol and analyzed by UHPLC/Q Exactive MS. Data was processed by CompoundDiscover. The major metabolic pathway catalyzed by the gut microbiota is ring fission leading to the formation of 5-dihydroxyphenyl valeric acid and its conjugates. J.B and P.D contributed equally to sample collection. P.D. analyzed data and made figure.

Table 3. 3. MCD-induced liver injury alters the cecum bacterial profile.

Bacteria Category	CD	CD+GTE	MCD	MCD+GTE	Overall Model p-Value
Phyla					
Unassigned_Other	0.0041 (0.0032)	0.0017 (0.0002)	0.0142 (0.0084)	0.0038 (0.0025)	0.8518
Actinobacteria	0.0006 (0.0003)	0.0005 (0.0001)	0.0051 (0.0013)	0.0051 (0.0031)	0.0002
Bacteroidetes	0.2226 (0.0448)	0.3234 (0.0329)	0.0592 (0.0194)	0.1251 (0.0312)	<0.0001
Cyanobacteria	0.0138 (0.0004)	0.0164 (0.0007)	0.0142 (0.0009)	0.0139 (0.0003)	0.0084
Deferribacteres	0.0303 (0.0095)	0.0562 (0.0052)	0.0261 (0.0087)	0.0412 (0.0120)	0.0188
Firmicutes	0.6858 (0.0600)	0.4338 (0.0390)	0.6507 (0.0361)	0.5914 (0.0484)	0.0014
Proteobacteria	0.0193 (0.0073)	0.0028 (0.0024)	0.0203 (0.0089)	0.0118 (0.0037)	0.0337
TM7	0.0135 (0.0002)	0.0132 (0.0000)	0.0132 (0.0000)	0.0135 (0.0001)	0.0132
Tenericutes	0.0075 (0.0018)	0.0077 (0.0021)	0.0454 (0.0106)	0.0369 (0.0071)	<0.0001
Verrucomicrobia	0.0289 (0.0172)	0.1706 (0.0339)	0.1781 (0.0362)	0.1835 (0.0385)	<0.0001
Class					
Actinobacteria_Coriobacteriia	0.0137 (0.0003)	0.0137 (0.0001)	0.0158 (0.0006)	0.0143 (0.0003)	0.0006
Bacteroidetes_Bacteroidia	0.2226 (0.0448)	0.3234 (0.0329)	0.0591 (0.0194)	0.1251 (0.0312)	<0.0001
Cyanobacteria_4C0d.2	0.0138 (0.0004)	0.0164 (0.0007)	0.0133 (0.0001)	0.0136 (0.0002)	<0.0001
Deferribacteres_Deferribacteres	0.0303 (0.0095)	0.0562 (0.0052)	0.0261 (0.0087)	0.0412 (0.0120)	0.0188
Firmicutes_Bacilli	0.0136 (0.0069)	0.0012 (0.0005)	0.2424 (0.0399)	0.0913 (0.0201)	<0.0001
Firmicutes_Clostridia	0.6425 (0.0594)	0.4092 (0.0377)	0.3451 (0.0308)	0.4322 (0.0471)	<0.0001
Proteobacteria___Deltaproteobacteria	0.0311 (0.0071)	0.0155 (0.0023)	0.0147 (0.0006)	0.0132 (0.0000)	0.01
Proteobacteria_Gammaproteobacteria	0.0008 (0.0003)	0.0004 (0.0001)	0.0167 (0.0073)	0.0115 (0.0037)	0.0021
Tenericutes_Mollicutes	0.0075 (0.0018)	0.0077 (0.0021)	0.0454 (0.0106)	0.0369 (0.0071)	<0.0001
Verrucomicrobia_Verrucomicrobiae	0.0289 (0.0172)	0.1706 (0.0339)	0.1781 (0.0362)	0.1835 (0.0385)	<0.0001

Table 3. 3. (Continued).

Bacteria Category	CD	CD+GTE	MCD	MCD+GTE	Overall Model p-Value
Order					
Actinobacteria___Coriobacteriales	0.0137 (0.0003)	0.0137 (0.0001)	0.0158 (0.0006)	0.0143 (0.0003)	0.0006
Bacteroidetes____Bacteroidales	0.2226 (0.0448)	0.3234 (0.0329)	0.0591 (0.0194)	0.1251 (0.0312)	<0.0001
Cyanobacteria_4C0d.2_YS2_	0.0303 (0.0095)	0.0562 (0.0052)	0.0261 (0.0087)	0.0412 (0.0120)	0.0188
Deferribacteres__Deferribacterales	0.0140 (0.0006)	0.0132 (0.0000)	0.0258 (0.0067)	0.0134 (0.0001)	0.0322
Firmicutes__Bacillales	0.0109 (0.0053)	0.0009 (0.0004)	0.0271 (0.0105)	0.0135 (0.0075)	0.0043
Firmicutes___Lactobacillales	0.0018 (0.0012)	0.0003 (0.0000)	0.2021 (0.0378)	0.0775 (0.0159)	<0.0001
Firmicutes___Turicibacterales	0.6425 (0.0594)	0.4092 (0.0377)	0.3451 (0.0308)	0.4322 (0.0471)	<0.0001
Firmicutes___Clostridiales	0.0311 (0.0071)	0.0155 (0.0023)	0.0147 (0.0006)	0.0132 (0.0000)	0.01
Proteobacteria_Desulfovibrionales	0.0008 (0.0003)	0.0004 (0.0001)	0.0167 (0.0073)	0.0115 (0.0037)	0.0025
Proteobacteria__Enterobacteriales	0.0075 (0.0018)	0.0074 (0.0021)	0.0448 (0.0106)	0.0358 (0.0073)	<0.0001
Tenericutes__RF39	0.0289 (0.0172)	0.1706 (0.0339)	0.1781 (0.0362)	0.1835 (0.0385)	<0.0001
Verrucomicrobia_Verrucomicrobiales	0.0137 (0.0003)	0.0137 (0.0001)	0.0158 (0.0006)	0.0143 (0.0003)	0.0006
Family					
Actinobacteria_Coriobacteriaceae	0.2106 (0.0421)	0.3195 (0.0307)	0.0573 (0.0195)	0.1169 (0.0273)	<0.0001
Bacteroidetes_Porphyromonadaceae	0.0138 (0.0004)	0.0164 (0.0007)	0.0133 (0.0001)	0.0136 (0.0002)	<0.0001
Bacteroidetes____Rikenellaceae	0.0303 (0.0095)	0.0562 (0.0052)	0.0261 (0.0087)	0.0412 (0.0120)	0.0188
Deferribacteres__Deferribacteraceae	0.0132 (0.0000)	0.0132 (0.0000)	0.0134 (0.0001)	0.0132 (0.0000)	0.0012
Firmicutes____Bacillaceae	0.0140 (0.0006)	0.0132 (0.0000)	0.0254 (0.0066)	0.0133 (0.0001)	0.0384
Firmicutes____Staphylococcaceae	0.0056 (0.0025)	0.0008 (0.0004)	0.0107 (0.0028)	0.0132 (0.0075)	0.0071
Firmicutes____Lactobacillaceae	0.0018 (0.0012)	0.0003 (0.0000)	0.2021 (0.0378)	0.0775 (0.0159)	<0.0001
Firmicutes____Turicibacteraceae	0.0225 (0.0192)	0.0024 (0.0013)	0.1081 (0.0224)	0.0543 (0.0138)	<0.0001

Table 3. 3. (Continued).

Bacteria Category	CD	CD+GTE	MCD	MCD+GTE	Overall Model p-Value
Firmicutes____Clostridiaceae	0.0841 (0.0141)	0.0700 (0.0053)	0.0545 (0.0074)	0.0990 (0.0188)	0.0344
Firmicutes____Lachnospiraceae	0.0134 (0.0002)	0.0132 (0.0001)	0.0142 (0.0002)	0.0132 (0.0000)	0.0002
Firmicutes___Peptostreptococcaceae	0.2583 (0.0531)	0.1932 (0.0368)	0.0959 (0.0209)	0.1597 (0.0212)	0.0112
Firmicutes____Ruminococcaceae	0.0136 (0.0002)	0.0135 (0.0001)	0.0134 (0.0001)	0.0144 (0.0004)	0.0019
Firmicutes____.Mogibacteriaceae.	0.0311 (0.0071)	0.0155 (0.0023)	0.0147 (0.0006)	0.0132 (0.0000)	0.0099
Proteobacteria__Desulfovibrionaceae	0.0008 (0.0003)	0.0004 (0.0001)	0.0167 (0.0073)	0.0115 (0.0037)	0.0025
Proteobacteria__Enterobacteriaceae	0.0289 (0.0172)	0.1706 (0.0339)	0.1781 (0.0362)	0.1835 (0.0385)	<0.0001
Verrucomicrobia_Verrucomicrobiacea	0.0137 (0.0003)	0.0137 (0.0001)	0.0158 (0.0006)	0.0143 (0.0003)	0.0006
Genus					
Actinobacteria____Adlercreutzia	0.2106 (0.0421)	0.3195 (0.0307)	0.0573 (0.0195)	0.1169 (0.0273)	<0.0001
Bacteroidetes____Parabacteroides	0.0248 (0.0050)	0.0169 (0.0038)	0.0145 (0.0007)	0.0171 (0.0024)	0.2116
Deferribacteres____Mucispirillum	0.0303 (0.0095)	0.0562 (0.0052)	0.0261 (0.0087)	0.0412 (0.0120)	0.0188
Firmicutes____Anaerobacillus	0.0132 (0.0000)	0.0132 (0.0000)	0.0133 (0.0001)	0.0132 (0.0000)	0.0085
Firmicutes____Lactobacillus	0.0056 (0.0025)	0.0008 (0.0004)	0.0107 (0.0028)	0.0132 (0.0075)	0.0071
Firmicutes____Turicibacter	0.0018 (0.0012)	0.0003 (0.0000)	0.2021 (0.0378)	0.0775 (0.0159)	<0.0001
Firmicutes____Clostridium	0.0132 (0.0000)	0.0132 (0.0000)	0.0133 (0.0001)	0.0133 (0.0001)	0.0108
Firmicutes____SMB53	0.0132 (0.0000)	0.0132 (0.0000)	0.0132 (0.0000)	0.0132 (0.0000)	0.0204
Firmicutes____Blautia	0.0132 (0.0000)	0.0136 (0.0001)	0.0132 (0.0000)	0.0142 (0.0004)	0.0008
Firmicutes____Coprococcus	0.0205 (0.0052)	0.0160 (0.0016)	0.0091 (0.0019)	0.0234 (0.0066)	0.0424
Firmicutes____Dorea	0.0008 (0.0002)	0.0015 (0.0003)	0.0013 (0.0006)	0.0040 (0.0007)	<0.0001
Firmicutes____.Ruminococcus.	0.0100 (0.0024)	0.0100 (0.0017)	0.0050 (0.0009)	0.0098 (0.0016)	0.0183

Table 3. 3. (Continued).

Bacteria Category	CD	CD+GTE	MCD	MCD+GTE	Overall Model p-Value
Firmicutes____Ruminococcus	0.0287 (0.0085)	0.0406 (0.0040)	0.0289 (0.0058)	0.0194 (0.0037)	0.0336
Proteobacteria____Bilophila	0.0310 (0.0070)	0.0155 (0.0023)	0.0147 (0.0006)	0.0132 (0.0000)	0.01
Proteobacteria____Desulfovibrio	0.0132 (0.0000)	0.0132 (0.0000)	0.0132 (0.0000)	0.0132 (0.0000)	0.0003
Proteobacteria____Klebsiella	0.0132 (0.0000)	0.0132 (0.0000)	0.0132 (0.0000)	0.0132 (0.0000)	0.0096
Verrucomicrobia___Akkermansia	0.0289 (0.0172)	0.1706 (0.0339)	0.1781 (0.0362)	0.1835 (0.0385)	<0.0001

Table 3. 3. MCD-induced liver injury alters the cecum bacterial profile. At the conclusion of the study, cecum samples were sent to Argonne National Laboratory where DNA extraction and 16S sequencing was performed and analyzed by the Quantitative Insights into Microbial Ecology (QIIME) program. Next, production of the PCR amplicon library, amplicon quantification and sequencing, and operation taxonomic units (OTUs) selection and filtration was conducted. For each type of bacteria, relative abundance means and standard errors were calculated for each group. *p*-value of <0.05 was considered significant. J.B. analyzed data and made figure with assistance from G.H. J.B.H. assisted with data analysis.

Figure 3.1. Experimental Design.

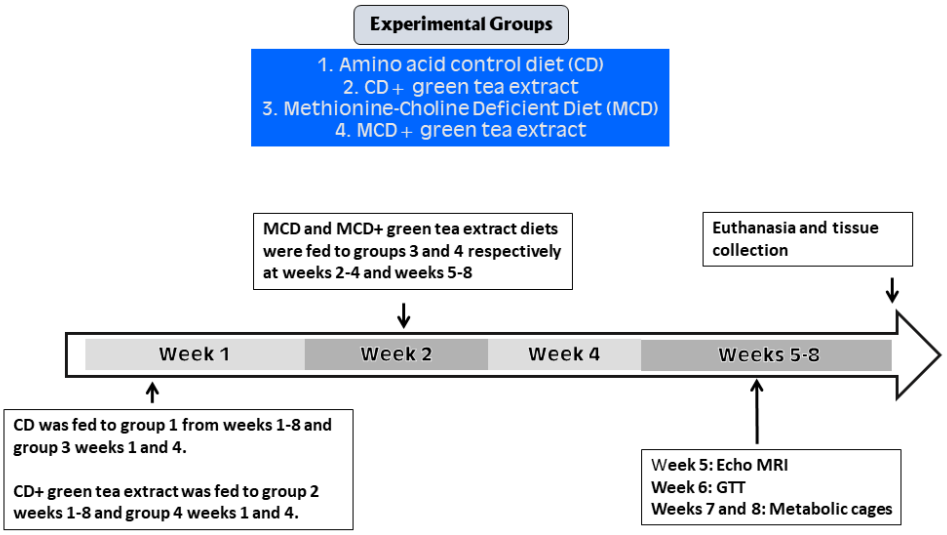

Figure 3.1. Experimental Design. Outline of the experimental groups, diet regimen, and study timeline. J.B. designed the study and timeline with consultation.

Figure 3.2. MCD feeding increases hepatic steatosis and inflammation.

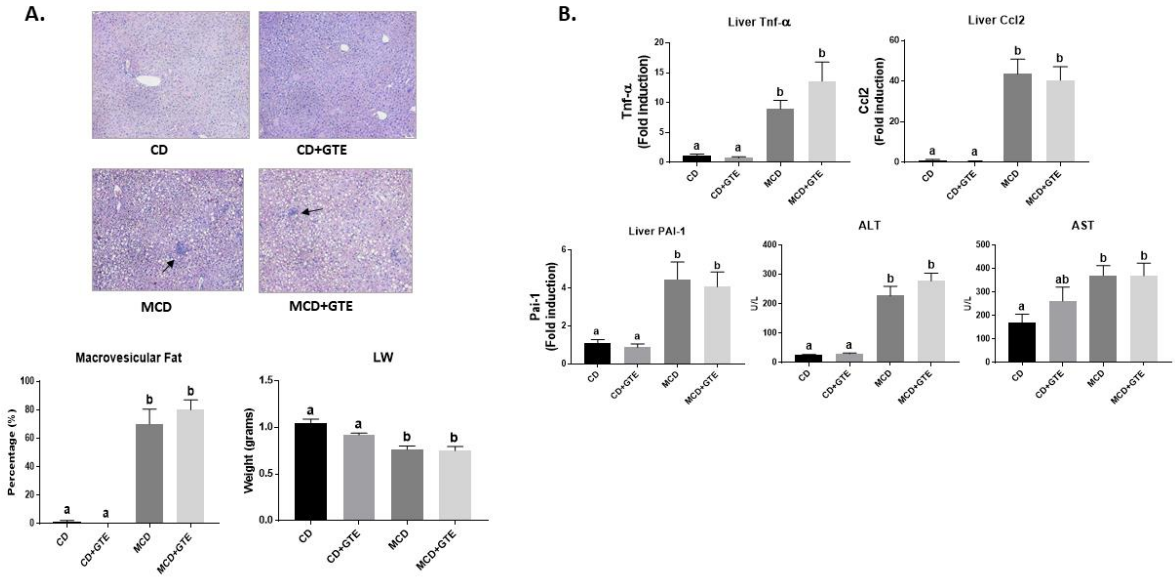

Figure 3.2. MCD feeding increases hepatic steatosis and inflammation. (A) H&E staining of liver sections. Each image is illustrative per treatment group. A liver pathologist determined the percentage of macro vesicular fat in H&E stained hepatic sections. Mice livers were weighed post euthanasia. (B) Hepatic mRNA expression of inflammatory genes *Tnf-α, Ccl2, and Pai-1* were measured. The plasma levels of ALT and AST were measured using the Piccolo Xpress Chemistry Analyzer. Values are mean ± SEM and different letters denote significant differences (p-value <0.05). J.B. performed data analysis and made figures. E.L. determined macrovesicular fat content.

Figure 3.3. MCD-induced liver injury alters the green tea metabolite profile.

A.

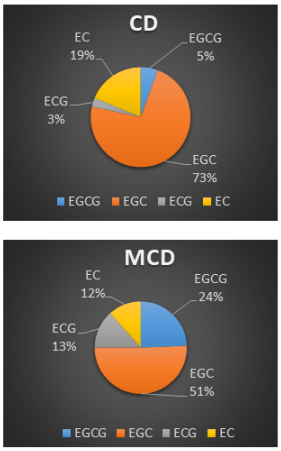

B.

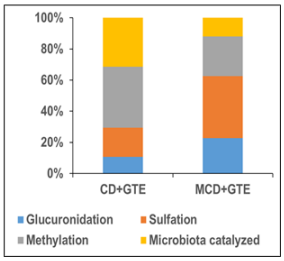

Figure 3.3. MCD-induced liver injury alters the green tea metabolite profile. At week 8, mice from each group were randomly selected (n=3) and placed into solo mice urine collection cages for 24 hours. (A) The metabolite profile of four flavan-3-ols, epigallocatechin gallate (EGCG), epicatechin gallate (ECG), epigallocatechin (EGC), and epicatechin (EC) assessed by UPLC-Q MS. (B) The percentage of phase 2 conjugation metabolites in the urine was determined. J.B and P.D contributed equally to sample collection. P.D. analyzed data and made figure.

Figure 3.4. Liver injury modifies expression of hepatic, not intestinal, phase 2 metabolizing enzymes.

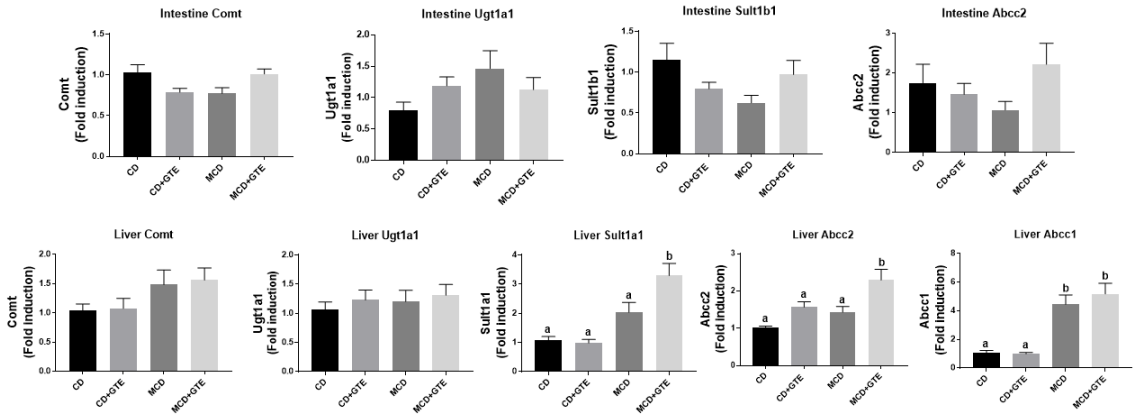

Figure 3.4. Liver injury modifies expression of hepatic, not intestinal, phase 2 metabolizing enzymes. The mRNA expression of intestinal and hepatic phase II metabolizing enzymes and transporters were measured using q-PCR. Values are mean ± SEM and different letters denote significant differences (p-value <0.05). J.B. conducted data analysis and made figures.

Figure 3.5. MCD-induced liver injury alters the bacterial phyla profile and the FB ratio.

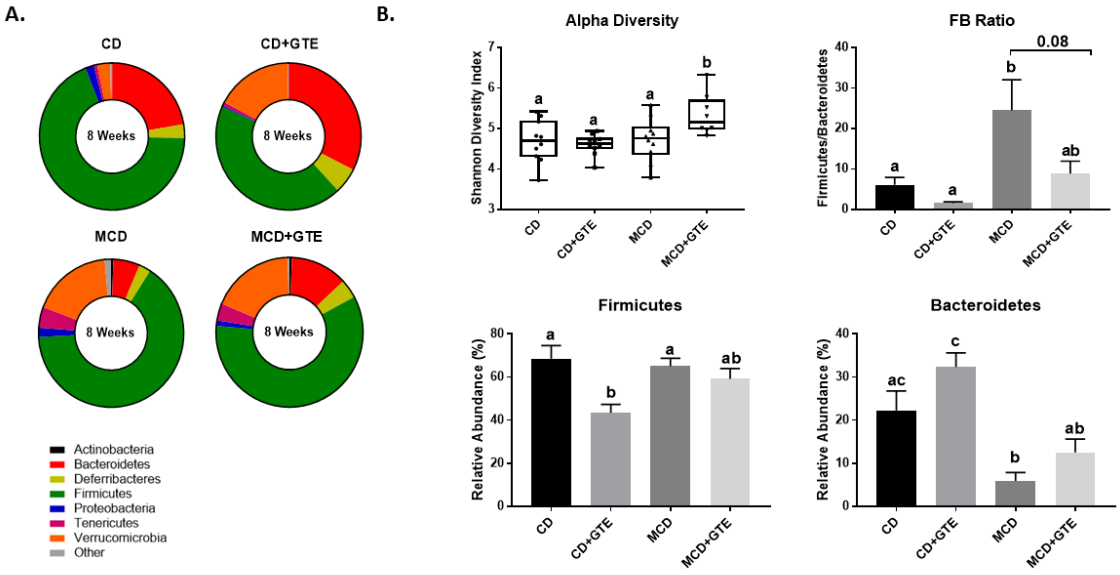

Figure 3.5. MCD-induced liver injury alters the bacterial phyla profile and the FB ratio. At the conclusion of the study, cecum samples were sent to Argonne National Laboratory for DNA extraction and 16S sequencing. Data was analyzed using QIIME. (A) Taxonomic composition of the cecal microbiota at the phylum level at sacrifice. (B) Alpha diversity was determined by Shannon Index. Data presented as percent relative abundances. Values are mean ± SEM and different letters denote significant differences (p-value <0.05). J.B. conducted data analysis and made figures. J.B.H. assisted with data analysis.

Figure 3.6. Liver injury causes gut dysbiosis via alterations in the cecal bacterial profile.

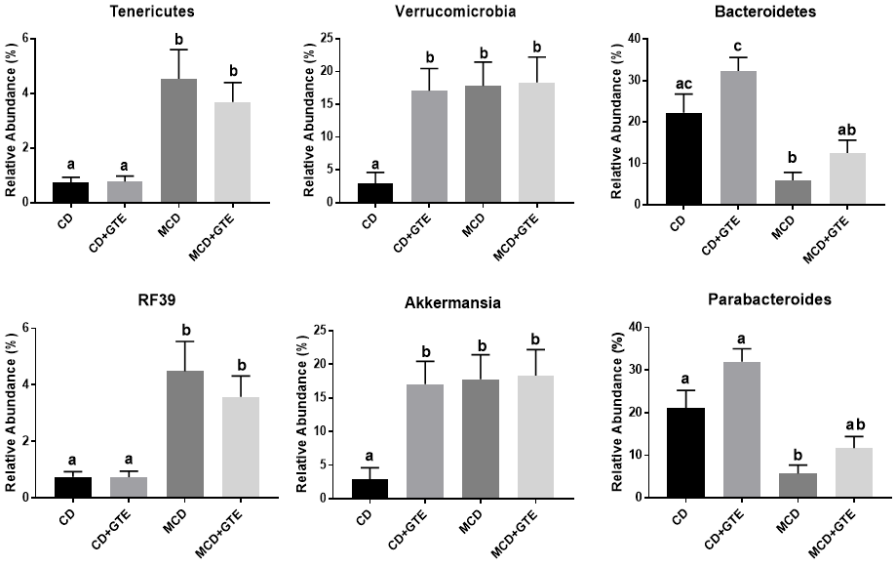

Figure 3.6. Liver injury causes gut dysbiosis via alterations in the cecal bacterial profile. The relative abundance of the phyla Tenericutes, Verrucomicrobia and Bacteroidetes and the corresponding order RF39, and genera Akkermansia and Parabacteroides respectively. Data presented as percent relative abundances. Values are mean ± SEM and different letters denote significant differences (p-value <0.05). J.B. conducted data analysis and made figures. J.B.H. assisted with data analysis.

Chapter 4 Specific Aim 3: Test the hypothesis that the prebiotic fiber inulin can attenuate steatohepatitis and PCB-126 toxicity in wild type C57BL/6 mice

Summary

Scope: Exposure to environmental pollutants, namely PCBs, have been linked to a variety of inflammatory diseases including CVD and NAFLD. Research has begun to elucidate the interplay between fatty liver disease and pollutant toxicity, although studies observing the effects in severe liver injury models are lacking. Additionally, the liver's intricate blood supply makes it susceptible to organ-organ system interactions, for example with the gut-microbiota. Previous studies in our lab showed that in the presence of a compromised liver, PCB toxicity and nutrient metabolism is altered, and the gut microbiota may play a major role in these results. Hence, this study sought to determine if prebiotic supplementation (inulin) can mitigate the effects of PCB-126 toxicity in a severe liver injury mouse model.

Methods and Results: In this 8 week study, C57BL/6 mice were fed a purified MCD diet with the fiber source either as 8% cellulose or 8% inulin (wt/wt). At week 4 of the study mice were gavaged with either vehicle corn oil or PCB-126 (0.5 mg/kg). Body weight was measured weekly. To assess body composition, EchoMRI was performed one week post PCB gavage (week 5) and at week 6 of the study, a GTT was performed to assess for glucose sensitivity. Post euthanasia blood and tissues samples were harvested for histological

examination and gene expression via q-PCR. H&E staining revealed that MCD-diet fed mice exhibited steatosis although there was no observable effects of PCB-126 or inulin on macrovesicular fat content. Interestingly, both inulin supplemented groups displayed a restoration in body weight loss when compared to their MCD-diet only fed counterparts. Additionally, the MCD+Inulin group had an increase in the body fat mass and decrease in the body lean mass when compared to all other groups, suggesting a restoration of the lean, wasting phenotype seen with MCD-diet. With regards to glucose metabolism, there were no relevant effects of PCB-126 or inulin in this study. Interestingly in both PCB-exposed groups, the AhR target Cyp1a1 was increased with inulin supplementation significantly decreasing Cyp1a1 expression.

Conclusions: Considering all of the findings in this study, inulin was able to restore body weight and body composition in this PCB exposed severe injury mouse model. Interestingly the observed inulin effects may be a result of interactions with the AhR signaling pathway. However, since these findings are preliminary, further analysis is warranted.

Introduction

Exposure to environmental pollutants have been implicated in the pathophysiology of many diseases. A specific class of persistent organic pollutants, PCBs, have been linked to the development of multiple chronic inflammatory diseases including atherosclerosis and NAFLD [32, 35]. Human exposure to PCBs are typically through consumption of contaminated food sources and there are a variety of mechanisms that has been proposed of how pollutant exposure can cause deleterious health outcomes and disease risk. Specifically, dioxin-like pollutants like PCB-126 can influence disease states by increasing inflammation and oxidative stress [89].

Previously, we showed that in mice with pre-existing liver injury, PCB-126 toxicity is worsened and exacerbates hepatic steatosis and inflammation as well as increased systemic inflammation [18]. In this same liver injury model, we also showed that nutrient metabolism was altered, possibly hindering the protective effects of GTE. An interesting finding in both these studies was that the gut microbiota may have contributed to these findings, as seen in Chapter 2 gut metabolites being excreted in liver injury mice simultaneously exposed to PCBs and the occurrence of gut dysbiosis in the MCD+GTE study of Chapter 3.

One way to combat the effects seen in this dissertation is by increasing consumption of foods that are rich in beneficial nutrients such as polyphenols and prebiotics. Since we observed changes in the liver and the gut microbiota in both chapters, we desired to utilize an intervention that could target both organs, hence the prebiotic inulin was chosen for this study. Prebiotics are any

“selectively fermented ingredient that allows specific changes, both in the composition and/or activity in the gastrointestinal microflora, that confers benefits” and play an important role in maintaining and influencing gut health [67]. In the food industry, inulin is a popular source for fiber supplementation and is one of the most ingested fiber components in the country, making it a practical means for intervention [117]. Also, recent research has shown that inulin has a major impact on multiple NAFLD-associated events such as body weight, body mass index, and serum levels of inflammatory and liver injury markers [71, 118]. Thus, inulin is a primary candidate for nutritional intervention in this mouse model.

Taken altogether, the primary objective of this present study was to determine the ability of the prebiotic inulin to protect against the development of steatohepatitis and block PCB-126 toxicity.

Experimental design and methods

Animals, diet, and experimental design

All aspects of this study were approved by the Institutional Animal Care and Use Committee at the University of Kentucky. Animals were housed in a light and temperature controlled room on a 12 hour light/dark cycle with food and water administered *ad libitum*. Eight week-old male C57BL/6 mice were purchased from Taconic (Hudson, NY, USA) and divided evenly into four experimental groups (n=10) during this 8-week study. During week 1 of the study,

mice were fed their respective control diets and at week 2, mice were fed a purified MCD diet with 8% cellulose as the source of fiber (MCD; TD.180883; Envigo) or a MCD diet with supplementation of the prebiotic inulin (Inulin; TD.180884; Envigo) at 8% (w/w) as the fiber source. Appropriate groups were orally gavaged with vehicle corn oil or PCB-126 (0.5 mg/kg) at week 4 of the study. To avert excessive weight loss and subsequent non-compliance with the approved IACUC protocol, all MCD mice were returned back to their respective control diets for one week (week 5) of this study.

Inulin supplementation and dosage information

Inulin was acquired from Beneo (Orafti® HP, Beneo). Inulin was supplemented into the MCD diet (TD.180883; Envigo) diet at 8% (w/w). The dosage of fiber selected for this study was chosen to mimic “high” fiber intake based on human dietary recommendations [65]. The customary level of fiber in purified rodent diets is 5% which equates to 12 grams per 1000 calories. The 8% of fiber used in this study can be considered as a “high” fiber diet as this equates to 21 grams per 1000 calories.

Hepatic histological sectioning and examination

At the completion of the study, liver tissues were immediately fixed in 10% neutral buffered formalin for 24-48 hours. The tissues were then sliced and hepatic sections were stained with hematoxylin and eosin (H&E) followed by examination by light microscopy. A liver pathologist assessed the stained

sections for macrovesicular fat percentage and inflammation. Reagents were obtained from Sigma-Aldrich Corp (St. Louis, MO, USA). Images were captured using a high resolution digital scanner at 10x magnification.

Measurement of body composition

Animals were analyzed via nuclear magnetic resonance spectroscopy (EchoMRI) for lean and body fat mass one week post PCB gavage (week 5) of the present study. In short, based on body weight, conscious mice were placed into breathable cylindrical plastic tubes. The mice inside the tubes were subsequently placed into a system that applies an external magnetic field and scanned for body composition.

Glucose Tolerance Testing

A glucose tolerance test (GTT) was conducted one week post PCB gavage (week 6) of the study. Mice were fasted during the light phase for 4-6 hours and glucose was administered via intraperitoneal injection (i.p.) at 1 mg glucose/grams body weight in sterile saline. Fasting blood glucose levels were determined via a hand-held glucometer (Freestyle Freedom Lite Abbott, Alameda, CA, USA) utilizing 1-2 µL of blood via the tail vein. Subsequent blood glucose levels were measured at 15, 30, 60, and 120 minutes post injection.

RNA extraction and q-PCR

Mouse liver and intestinal samples were homogenized using a bench top bead beater and total RNA was extracted using the TRIzol reagent (Invitrogen, Carlsbad, CA). The purity and concentrations of the mRNA was determined with the NanoDrop 2000/2000c (Thermo Fisher Scientific Inc., Waltham, MA, USA) using the NanoDrop 2000 software. Next, total RNA was used to synthesize complementary DNA using the QuantiTect Reverse Transcription Kit (Qiagen, Valencia, CA, USA) following manufacturer's protocols. Polymerase chain reaction (PCR) was performed on the CFX96 Touch Real-Time PCR Detection System (Bio-Rad, Hercules, CA, USA) using the Taqman Fast Advanced Master Mix (Thermo Fisher Scientific Inc.) to determine the expression of inflammatory and fibrotic markers. The mRNA levels for the liver were normalized to amount of *Actb*. Expression levels in the mice fed the MCD diet alone and administered vehicle were set at 1. The $2^{-\Delta\Delta Ct}$ method was utilized to calculate the differences in gene expression levels [88]. All primers used in this study were obtained from Taqman Gene Expression Assays (Thermo Fisher Scientific Inc.).

Statistical Analysis

Analyses for all data represented in this study were conducted and corresponding graphs were plotted using GraphPad Prism Version 7.02 for Windows (GraphPad Software, Inc., La Jolla, CA). Data are expressed as mean mean ± SEM. Multiple group data was compared using Two Way ANOVA (column factor: diet row factor: Inulin) followed by the Tukey's post-hoc test for

multiple comparisons. The results were considered to be statistically significant and with an observed p-value of < 0.05.

Results

4.1 Experimental Design

The experimental design for this study is presented in Figure 4.1.

4.2 MCD feeding induced steatosis with no PCB-126 or inulin effects

To examine steatosis in these mice, liver sections were stained with H&E. As expected, MCD-feeding caused an increase in the fat accumulation in the hepatocytes of all groups as seen by macrovesicular fat content. As determined by a liver pathologist, there were no observable PCB-126 or inulin effects in the mice with regards to steatosis (Figure 4.2). In addition, the LW/BW ratio was determined. We observed an increase in the LW/BW ratio in mice exposed to PCB-126, signifying toxicity. However inulin exerted no effects with regards to this parameter.

4.3 Inulin restored body weight, fat, and lean mass in MCD-diet fed mice

MCD-feeding produces a lean phenotype in which mice experiences a decrease in body weight over time. Interestingly, when compared to the MCD-diet only fed group, both groups with inulin supplementation exhibited a restoration of body weight loss as shown by a significant increase in the % increase body weight at the conclusion of the study (Figure 4.3). In addition to

the effects that were seen with body weight, the body composition was also measured via EchoMRI one week post PCB-126 gavage (Week 5). The MCD+Inulin group showed a significant increase in the body fat mass and a significant decrease in the body lean mass when compared to all other groups, suggesting a reversal of the lean, wasting phenotype caused by MCD-feeding (Figure 4.3).

4.4 PCB-126 and Inulin do not exert physiological effects on glucose sensitivity

When compared to other models of liver disease and injury, an atypical characteristic of the MCD-fed rodent model is that the mice displays a hypoglycemic phenotype. To determine the effects that PCB-126 and inulin has on this phenomenon, a glucose tolerance test was conducted at week 6 of this study. There was no significant differences between any of the groups with regards to the fasting blood glucose (Figure 4.4). Furthermore, we observed no PCB-126 effect with area under the curve (AUC), although there was an inulin effect ($p=0.0143$). Taken altogether, we can infer that there was no major physiologically relevant effects with PCB-126 or inulin on blood glucose in this study.

4.5 Inulin decreases AhR target gene Cyp1a1 mRNA levels with no effects on hepatic inflammation.

To further examine the effects that PCB-126 and/or inulin have on hepatic injury, we measured the gene expression of inflammatory and fibrotic markers. The MCD+PCB+Inulin group had an increase in the inflammatory Tnf-α when

compared to the MCD+Inulin alone group. Inulin also increased expression of Ccl2 when compared to the MCD alone group and the MCD+PCB group. Interestingly, both Timp-1 and Pai-1 were increased only in the MCD+PCB+Inulin group.

To examine if AhR activation was involved in our findings in this study, the gene expression of its downstream target Cyp1a1 was determined. As expected both PCB exposed groups exhibited a significant increase in Cyp1a1 expression. Interestingly, inulin supplementation in the PCB exposed groups caused a significant decrease in Cyp1a1 expression.

Discussion

PCB-126 exposure has been linked to multiple chronic inflammatory diseases, including NAFLD. Data obtained from the studies presented in chapters 1 and 2 showed that a compromised liver can alter PCB-126 toxicity and GTE metabolism, with implications that the gut-microbiota may play a role in both of these outcomes [18]. Since the liver and the gut were prominent players in our results, we decided to study a nutritional intervention that could impact both organs, in addition to combatting the effects of PCBs.

Inulin was chosen for use in this study for multiple reasons. Firstly, insulin has recently become a popular fiber supplementation source in the food industry, making it the one of the most ingested fibers in the U.S. with the average American consuming 1-4 grams of inulin-type fructans daily [117].This makes it a

readily accessible and feasible means of nutritional intervention. Secondly, emerging research suggests that inulin has beneficial host health effects. With regards to the research contained within this chapter, inulin has been shown to possess protective properties against the anthropometric, inflammatory, and oxidative parameters seen in patients with NAFLD such as decreasing body weight and body mass index in addition to decreasing serum levels of Tnf-α [71]. In another study, grades of NAFLD and serum levels of ALT and AST were all decreased in NAFLD patients administered a symbiotic yogurt containing inulin [118]. Studies in rodent of models of NAFLD also showed similar results when fed a natural dietary supplement containing inulin [72]. Interestingly, in other mouse models of NAFLD, inulin supplementation ameliorated hepatic steatosis [119, 120]. Therefore, inulin was selected for use in this study.

First, we sought to examine the effects that PCB-126 and inulin could exert in mice with compromised liver. As determined by a liver pathologist, there were no significant differences between any of the groups with regard to macrovesicular fat content (H&E staining). However, we did observe an increase in the LW/BW ratio, a marker of toxicity, in both groups exposed to PCB-126 although there was no inulin effect. This finding suggests that in mice with severe liver injury, toxicity is increased when exposed to PCB-126, which is consistent with our findings in chapter 2. Yet, inulin exerts no protective effects on steatosis in this study.

EchoMRI was performed one week post PCB gavage to further examine the effects of PCB-126 and inulin in this model. The MCD model is notorious for

producing a lean phenotype within mice, with animals exhibiting extreme weight loss while fed the diet [46]. As stated before, using mice with a lean phenotype that do not get obese is important for studies with lipophilic PCBs. As expected, mice fed the MCD diet displayed body weight loss over the course of the study as shown by the % increase in body weight over time. Interestingly, the MCD+Inulin group showed a restoration of body weight, body fat mass, and lean mass when compared to all other groups. Since most animal models of NAFLD typically are obese, to our knowledge this is the first report of inulin restoring body weight loss in animals with severe liver injury.

Since glucose metabolism plays an important role in the progression of NAFLD, we next conducted a GTT. There was no significant differences with any of the groups with regards to fasting blood glucose in this study. PCB-126 did not alter glucose levels, which was a similar finding to previous studies in our lab. Unfortunately, inulin did not exert any protective effects on glucose levels.

The gene expression of markers of inflammation and fibrosis were also examined. We observed an increase in Tnf-α in the MCD+PCB+Inulin group when compared to MCD+Inulin alone. In addition, inulin increased the gene expression of Ccl2 when compared to the MCD alone group and the MCD+PCB group. When compared to mice fed the MCD alone, PCB-126 exposure did not increase the expression of Tnf-α, Ccl2, Timp-1, or Pai-1 in this study, which is contrary to our findings in chapter 2. It may be that the PCB-126 exacerbated effects were not yet pronounced with regards to these specific genes since the study presented in this chapter was conducted over 8 weeks while the study in

chapter 2 was a 14-week study. An interesting finding was that both Timp-1 and Pai-1 were increased only in the MCD+PCB+Inulin group when compared to all other groups. Timp-1 is a tissue inhibitor of metalloproteinases that is upregulated by inflammatory cytokines in NAFLD while Pai-1 is a major regulator of fibrosis and has been implicated in obesity-induced NAFLD pathogenesis [121, 122]. Although not many studies have examined the role of Timp-1 or Pai-1 in end stage liver injury, studies have shown that pharmacological inhibition of Pai-1 can reduce hepatic steatosis in MCD-diet fed mice but had not effect on inflammation or fibrosis [123]. This finding was contrary to our hypothesis that inulin is protective in NAFLD. However, since there were only four genes associated with inflammation and fibrosis tested in this study currently, it is premature to draw that conclusion. Thus, future analysis will be conducted to confirm the results.

To examine if activation of the AhR contributed to our findings in this study, q-PCR was conducted to measure the gene expression of the downstream AhR target Cyp1a1. As expected, both groups exposed to PCB-126 had a significant increase in Cyp1a1 gene expression. Interestingly, inulin supplementation decreased Cyp1a1 expression when compared to the MCD+PCB group alone although both groups were administered the same amount of PCB-126 (0.5 mg/kg). No other studies have reported an inulin specific decrease in Cyp1a1. One study showed that in high-fat and high sucrose-diet fed NAFLD rats, Cyp1a1 was decreased and inulin alleviated this reduction, however these rodents were not exposed to the AhR activating PCB-

126 [120]. Nonetheless, we and others have observed that inulin can alter the expression of Cyp1a1, suggesting that inulin's effects may be a result of its ability to interact with the AhR pathway. However, further studies would need to be conducted to tease out this mechanism.

Taken altogether, the findings in this study shows that inulin can restore body weight and body composition in this MCD mouse model. In addition, the effects seen with inulin may be associated with alterations in the AhR signaling pathway. However, these findings are preliminary and further analysis would need to be conducted to confirm these results.

Figure 4.1 Experimental design.

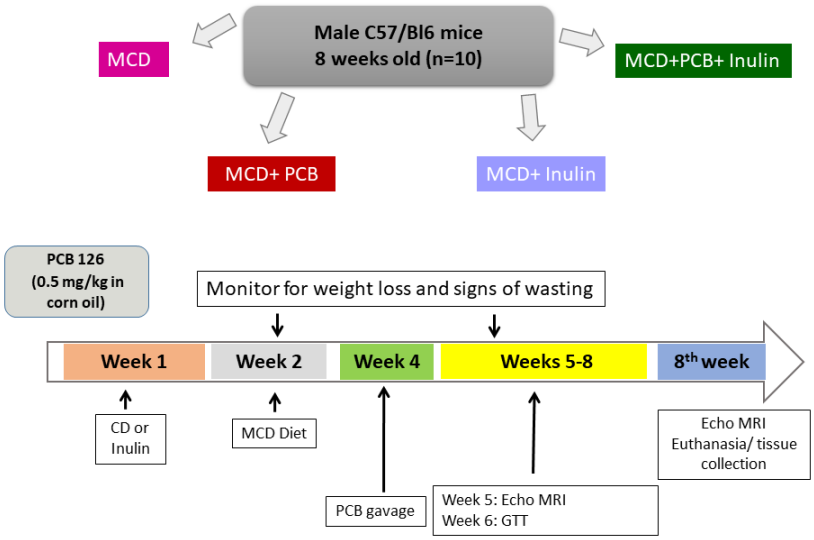

Figure 4.1 Experimental design. Mice were divided into 4 study groups (n=10) based on Inulin supplementation and PCB126 exposure. The timeline for diet separation and PCB exposure regimen are also outlined in the figure. J.B. designed the study and timeline with consultation.

Figure 4.2 MCD feeding induced steatosis with no PCB-126 or inulin effects.

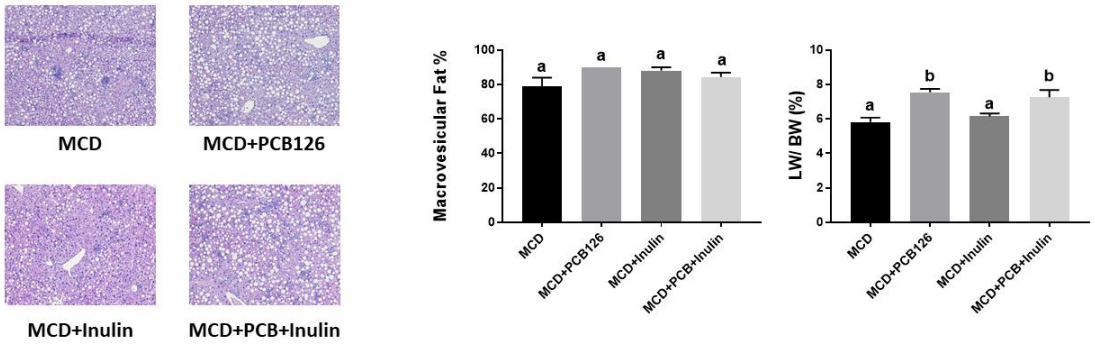

Figure 4.2 MCD feeding induced steatosis with no PCB-126 or inulin effects. Post euthanasia hepatic sections were stained with H&E. Macrovesicular fat content was determined by a liver pathologist. Each image is illustrative per treatment group. Mice livers were weighed post euthanasia and the liver to body weight ratio was calculated. Values are mean ± SEM and different letters denote significant differences (p-value <0.05). J.B. conducted data analysis and made figures. E.L. determined macrovesicular fat content.

4.3 Inulin restored body weight, fat, and lean mass in MCD-diet fed mice.

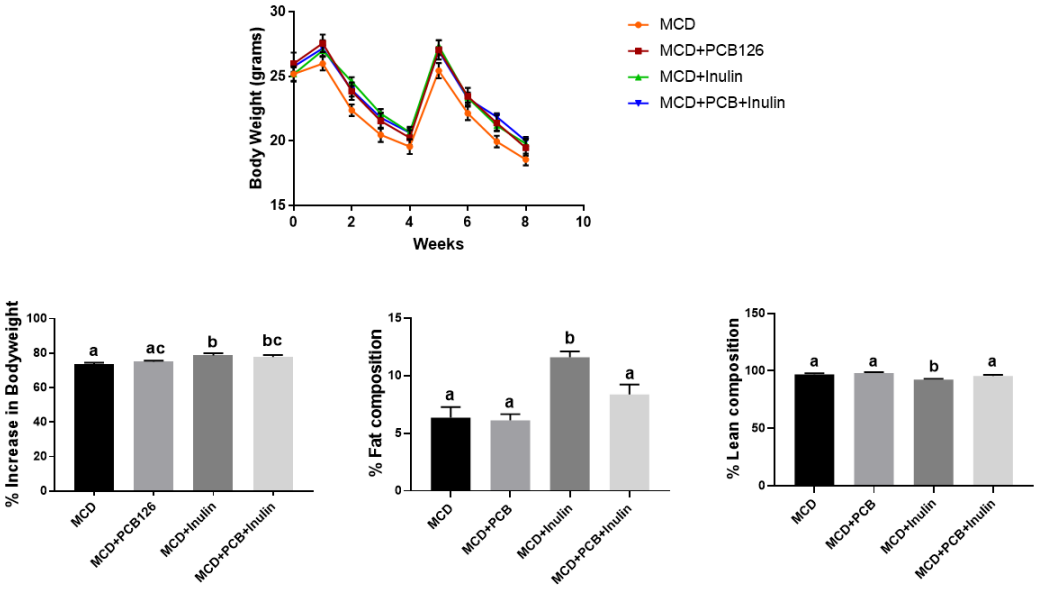

4.3 Inulin restored body weight, fat, and lean mass in MCD-diet fed mice.

The % increase in BW was calculated and the BW at week 1 was taken as 100%. Body mass composition was determined by EchoMRI at week 5 of the study. Values are mean ± SEM and different letters denote significant differences (p-value <0.05). J.B. conducted data analysis and made figures.

4.4 PCB-126 and Inulin do not exert physiological effects on glucose sensitivity.

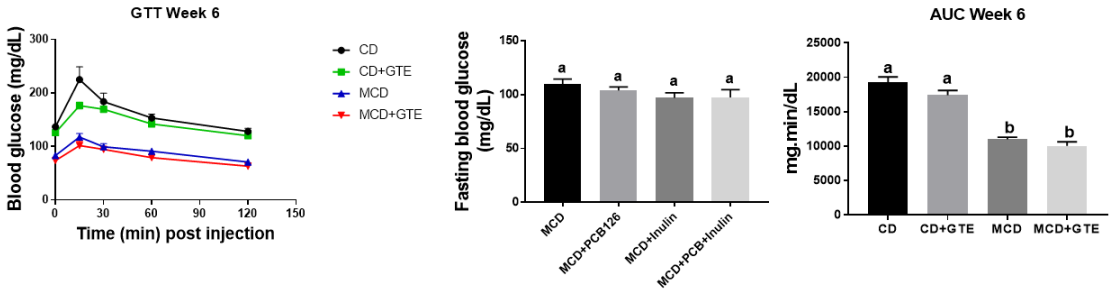

4.4 PCB-126 and Inulin do not exert physiological effects on glucose sensitivity. A glucose tolerance test was performed at week 5 of the study. Mice were fasted for 4-6 hours and fasting blood glucose levels (mg/dL) were measured prior to the testing with a handheld glucometer (Freestyle Freedom Lite Abbott, Alameda, CA, USA) using 1-2 µL of blood via the tail vein. Glucose was given via intraperitoneal injection (i.p.) at 1 mg glucose/grams body weight in sterile saline and blood glucose levels were measured at 15, 30, 60, and 120 minutes post injection. Values are mean ± SEM and different letters denote significant differences (p-value <0.05). J.B. conducted data analysis and made figures.

4.5 Inulin decreases AhR target gene Cyp1a1 with no effects on hepatic inflammation.

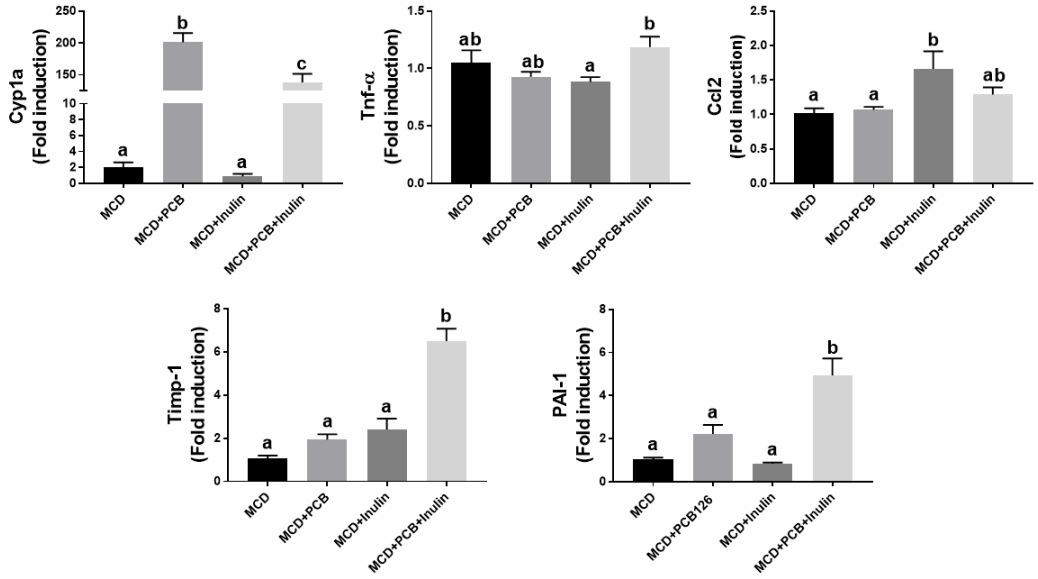

4.5 Inulin decreases AhR target gene Cyp1a1 with no effects on hepatic inflammation. The mRNA expression of AhR target gene Cyp1a1 and inflammatory and fibrotic genes Tnf-α, Ccl2, Timp-1, and Pai-1 were determined via q-PCR. The mRNA levels for the liver were normalized to amount of *Actb*. Expression levels in the mice fed the MCD diet alone and administered vehicle were set at 1. Values are mean ± SEM and different letters denote significant differences (p-value <0.05). J.B. conducted data analysis and made figures.

Chapter 5: Overall Discussion

Summary

The general public's exposure to pollutants like PCB-126 is still a significant health concern with detectable levels of these contaminants currently seen in human populations long after the banishment of these chemicals for industrial use [124, 125]. Unfortunately, every organ system in the human body can be impacted by pollutant exposure. PCBs also have been linked to multiple disease pathologies although the mechanisms of actions both at the cellular level and systemically are in general still unclear or inconclusive, proving that studies are still needed to be conducted to increase our knowledge and gain better understanding. There are variety of epidemiological studies linking pollutant exposure to NAFLD. For example, Cave et al. demonstrated an association between PCBs and increased levels of the plasma liver injury marker ALT, suggesting a correlation between pollutant exposure and NAFLD [35]. Additionally, with current therapeutic strategies to attenuate and even abolish NAFLD mainly focused on dietary and lifestyle interventions, it is important to understand how a compromised liver can alter the intentional beneficial effects of diet-derived nutrients.

The primary objective of the research contained in this dissertation was to determine how toxicity of PCBs is changed in individuals with severe liver injury and how beneficial nutrition can attenuate these effects. In chapter 2, we demonstrated that indeed PCB-126 toxicity is worsened in the presence of a compromised liver, with implications of the gut microbiota and its derived

metabolites (e.g. TMAO) in CVD risk. In chapter 3, we sought to understand if GTE could attenuate steatohepatitis null PCB-126 and we saw that surprisingly, GTE at the dose used in this study was not protective against severe liver injury in MCD-fed mice. However, it was also determined that in the presence of a compromised liver, mice have gut dysbiosis and simultaneously GTE metabolism is altered. This suggests that a compromised gut-liver axis can influence GTE metabolism in a negative way and possibly decrease the therapeutic effects of bioactive nutrients. With all this in mind, the study in chapter 3 sought to determine if a nutrient that has the ability to act on both the liver and the gut microbiota, the prebiotic inulin, can attenuate the effects of steatohepatitis in this liver injury mouse model. While the findings of this study are preliminary, we have evidence to support the notion that in MCD-fed mice, inulin can restore body weight and body composition and its effects may involve interactions with the AhR pathway. However, further analysis is needed to determine the direct effects that inulin plays in hepatic, systemic, and gut microbiota toxicity.

Aim 1: A compromised liver worsens PCB-126 toxicity: Implications for the role of the gut microbiota

There are a variety of epidemiological and animal studies that support the idea that dioxin-like pollutants, like PCB-126, are linked to the development and/or progression of chronic inflammatory disease [55, 126-129]. The mechanisms of actions that may contribute to these disease pathologies involve the chronic activation of the AhR by ligand binding of co-planar PCBs, causing

oxidative stress and increased inflammation in both the target organs and peripheral vasculature [130]. In particular, it has been shown that dioxin-like pollutants are associated with NAFLD in rodent and clinical models [35, 80]. Although all of the above is true, it is not completely clear what role a compromised liver plays on PCB-126 toxicity and associated disease risks. The research described in chapter two of this dissertation tried to answer this literature gap by examining the effects of severe liver injury on PCB-126 toxicity in mice.

The selection of the rodent model used in the studies presented in this dissertation was important. We decided to use the MCD-diet to induce liver injury and study PCB effects for two main reasons. Firstly, we desired to use a diet-derived mouse model that closely mimicked end stage liver disease. Secondly, ensuring that the mice did not become obese was crucial to studies including PCBs, as it has been shown that individuals can be protected from PCB effects during a weight loss phase [55]. In chapter 2, we determined that MCD-diet fed mice exposed to PCB-126 had worsened steatosis as determined by H&E staining, increased levels of plasma liver injury markers, and increased gene expression of inflammatory and fibrotic markers in the liver. As expected, we saw increased expression of the AhR target Cyp1a2 in both groups exposed to PCB-126. Additionally, since recent literature has implicated the metabolite TMAO in CVD risk, we examined the effects that PCB-126 may exert on the levels of this molecule in our compromised liver model. Interestingly, hepatic Fmo3 and both hepatic and plasma TMAO was increased solely in the MCD+PCB-126 group.

This is important as it not only implicates pre-existing liver injury in the increased risk of PCB-126 associated CVD, but also suggests that the gut microbiota plays an important role in PCB-associated inflammatory disease pathology since TMAO is derived from actions of the gut and the liver. Finally, we proved that MCD+PCB-126 mice had increased levels of early markers of endothelial cell dysfunction and inflammatory cytokines. Taken altogether, the findings presented in chapter 2 provided novel evidence that suggests a compromised liver can exacerbate hepatic and systemic PCB-126 toxicity, with implications that the gut microbiota plays a major role in chronic inflammatory disease, specifically CVD, risk. Therefore, focusing research on determining the effects of the gut-liver axis on pollutant toxicity is important, in addition to finding therapeutic methods to attenuate these effects such as nutritional intervention with beneficial nutrients.

Aim 2: GTE does not protect against steatohepatitis: Implications of the gut-liver axis on nutrient metabolism

Based on our findings from chapter 2 we then decided to study how nutritional intervention could mitigate the effects we observed. Previous studies in our lab and others have shown that GTE and its major metabolite EGCG can protect against pollutant induced-inflammatory outcomes and diseases including inflammation in endothelial cells and NAFLD [64, 95]. The mechanisms of action typically associated with this attenuation is through the anti-oxidant and anti-inflammatory properties of GTE and its components, which acts on the same pathways that pollutants like dioxin-like PCBs target. However, the extent that

which GTE can protect against severe NAFLD is not well understood with most studies utilizing less severe animal models. As stated previously, it is important to study rodent models that mimic end stage liver injury, as 25% of those diagnosed with NAFLD eventually progress and are diagnosed with the more severe disease state. Additionally, the concomitant effects of GTE supplementation and PCB-126 in this MCD model is uncertain, thus we decided to conduct a study without PCB-126. Therefore, in chapter 3, severe liver injury was induced in mice through MCD-diet feeding and GTE was supplemented into the diet at the achievable 1% wt/wt in diet (~4 cups of tea or ~200 mL/cup per day). GTE did not decrease steatosis as determined by the quantification of macrovesicular fat content nor did it decrease the MCD-induced hepatic inflammation and injury as seen by unchanged gene expression levels and ALT and AST plasma levels. To our surprise, based on the finding listed above it was determined that GTE does not protect against MCD-induced steatohepatitis in this mouse model.

We then desired to determine an explanation for these findings. There are studies that have investigated and proven that severe liver injury can alter the metabolism of endogenous and exogenous molecules and can subsequently change the efficacy and bioavailability of these components. Hence, a similar phenomenon may the reason we did not see protection in this model. Urine samples from the mice in this study were collected at week 8. Interestingly, we observed a significant change in the GTE metabolite profile in MCD diet fed mice. Specifically, an increase in glucuronidation and sulfated metabolites and a decrease in the methylation and gut-microbiota catalyzed metabolites were

observed. To further examine the mechanisms associated with these metabolism alterations the gene expression of intestinal and hepatic transporters and phase 2 metabolizing enzymes, in addition to the cecum microbiota profile were investigated. There were no significant changes in the intestinal gene expression for Comt, Ugt1a1, Sultb1, or Abbc2. We also observed no changes in hepatic Comt or Ugt1a1. However, expression of hepatic Sult1a1 and Abcc2 was significantly increased when compared to all other groups and the hepatic Abcc1 was increased in both MCD-diet fed groups. Remarkably, a complete alteration in the cecum gut microbiota profile was seen in MCD groups as seen by changes in the taxonomic composition at phyla, order, family, and genus levels, signifying gut dysbiosis.

Overall, the findings from chapter 3 displayed that GTE does not protect against MCD-diet induced liver injury. However, this lack of protection may be due to the fact that in the presence of a compromised liver, the GTE metabolite profile is altered, namely via changes in glucuronidation, sulfation, methylation, and gut-microbiota derived metabolites. Additionally, results produced from this model implicates the gut microbiota in disease risk, as gut dysbiosis was observed in this compromised liver mouse model, possibly contributing to the effects seen in GTE alterations.

Aim 3: Inulin restores body weight and composition with possible interactions with the AhR signaling pathway

In chapters 2 and 3 we saw that in mice with a compromised liver, PCB toxicity and nutrient metabolism (GTE) was altered, with a possible role of the gut microbiota. Therefore, in the study contained in chapter 4, we investigated if the prebiotic inulin could attenuate the deleterious effects of PCB-126 toxicity in a severe liver injury mouse model. In this 8 week study, male C57Bl/6 were fed a purified MCD diet with the fiber source either 8% cellulose or 8% inulin (wt/wt). The 8% inulin used in this study can be considered a “high” fiber diet. Appropriate groups were administered PCB-126 at 0.5 mg/kg via oral gavage at week 4.

Inulin did not protect against MCD-induced liver injury while PCB-126 in both groups caused toxicity as seen by a significant increase in the LW/BW ratio. Interestingly as seen EchoMRI conducted one week post PCB gavage, inulin restored body weight and body composition by increasing the % increase body and fat mass and decreasing lean mass. To our knowledge this is the first report of inulin restoring body weight loss in animals with severe liver injury. This finding may be a result of inulin’s effects on PCB metabolism, although further studies would need to be conducted to evaluate this possibility.

Additionally, a GTT was conducted to assess glucose metabolism and sensitivity. No significant differences were seen with any of the groups for fasting blood glucose and PCB-126 did not alter glucose levels, a similar finding to a

previous study in our lab. With regards to inulin, we observed no protective effects on glucose homeostasis.

We then sought to examine hepatic inflammation in these mice. Tnf-α was increased in the MCD+PCB+Inulin group when compared to the MCD+Inulin group. Inulin increased the expression of Ccl2 when compared to the MCD alone and the MCD+PCB group. Contrary to our previous findings, PCB-126 did not have any effect on Tnf-α, Ccl2, Timp-1, or Pai-1. We speculate that PCB-126 effects were not yet pronounced with these specific genes because of a difference in the study timeline of the current study and our previously published work (8 weeks vs 14 weeks). In the MCD+PCB+Inulin group both fibrotic markers Timp-1 and Pai-1 were increased when compared to all the other groups. This suggests that inulin and PCB-126 increases fibrosis, which is contrary to our hypothesis.

With regards to AhR activation, not surprisingly both PCB-126 treated groups exhibited an increase in Cyp1a1 gene expression. However, prebiotic inulin supplementation decreased the gene expression of Cyp1a1 when compared to the MCD+PCB group alone. To our knowledge this is unique to our study as no other studies have reported an inulin specific decrease in Cyp1a1. These findings suggests that inulin's effects may be because of its ability to interact with the AhR pathway, although additional mechanistic studies would need to be done. Overall the findings from chapter 4 displayed that inulin restores body weight and composition in mice with pre-existing liver injury and

these effects may be associated with the AhR signaling pathway. However, further analysis is warranted as the findings in this study are preliminary.

Limitations

Although the data presented in this dissertation adds to the growing body of evidence implicating the gut-liver axis in toxicant, nutrient and overall metabolism and health, no study is without limitations.

The use of MCD-diet as a way to induce and study fatty liver disease is definitely something to consider, both for its ability to mimic human liver disease and within the context of this work. Since all patients with liver disease have the possibility of progressing to the far right end of the spectrum and 25% actually being diagnosed with end stage live disease, it is important to use a model that has the ability to generate a similar phenotype, hence the utilization of the MCD mouse model in these studies. In addition, there is animal studies and epidemiological evidence that supports the notion that leaner individuals may be more susceptible to the effects of lipophilic contaminants like dioxin-like PCBs because of the increased body burden of the pollutant from the lack of sequestration into the adipose tissue. For example, Baker et al. reported that mice with large fat depots due to weight gain were protected against the harmful effects of dioxin-like chemicals, while during a weight loss phase the mice demonstrated PCB-induced inflammation and glucose intolerance [55].

However, although it is a robust model and produces a phenotype similar to human NASH, the MCD diet has recently been criticized for its lack of

metabolic characteristics that are traditionally seen in patients with fatty liver disease such as obesity and hyperglycemia. Although this is true and should be considered when using this model to mimic human disease, interestingly, recent literature has shown that in mice choline deficiency can occur under pathophysiological conditions as high fat diets can lead to the formation of gut bacteria that convert dietary choline to methylamines. This consequently reduces the systemic plasma phosphatidylcholine levels, generating a phenotype similar to the NASH producing choline-deficient diets.[131] Regardless, the use of other diet-induced liver injury mouse models, like the high fat diet (HFD), may be useful to compare and contrast the findings obtained in this dissertation.

Another minor limitation that occurs in all of the studies presented in this dissertation is that the MCD diet fed mice were reverted back to their respective control diets for one week. As stated in above, this measure was taken to avoid excessive weight loss in these animals and subsequent non-compliance with our approved IACUC protocol. Although this resulted in a slight attenuation in the body weight loss of MCD diet fed mice, this does not cause a total recovery from the steatohepatitis that was observed, as confirmed by histological analysis post euthanasia. In fact, the reversal of MCD-induced hepatic effects typically occurs from 2-3 weeks of feeding a control diet [132].

Lastly, the use of solely male mice does not account for any sex differences that may contribute to the findings. In point of fact, data obtained from the National Health and Nutrition Examination Survey displayed that individuals with NAFLD were more likely to be male, suggesting a sex disparity in regards to

this particular disease [133]. Since both the severity of liver disease and the gut microbiota may differ between sexes, future studies would need to include female mice to examine the contribution that gender may have on the changes that were observed [134, 135].

Future Directions

There are variety of directions to take with future studies and the options are endless. Firstly, in chapter 2, since we observed increases in markers early endothelial cell dysfunction, it may be worthwhile to verify CVD risk and development in atherosclerotic animal models. Additionally, with the possible effects of the gut-microbiota seen in studies presented in chapters 2 and 3, teasing out the mechanisms that cause the gut-liver axis to exert its effects may be a next step, which would include the use of germ free mice or antibiotic treatment. Additionally, using other animal models of liver injury to compare our results would be of interest including a high fat or high-sucrose diet.

The study presented in chapter 4 has a lot of potential. Analysis of the gut microbiota profile could help gain a better understanding of its role in PCB mediated toxicity and inulin protection. In addition, no systemic inflammatory markers were measured as of yet, so obtaining plasma ALT, AST, and cytokine data would help to determine if PCB-126 exacerbates inflammation and liver injury in this model or if inulin has any protective effects. In addition, since we observed alterations in the expression of genes downstream the AhR, studies

looking into whether inulin can impact other targets of the pathway or even interact with AhR itself.

In conclusion, the data within this dissertation demonstrates that in the presence of a compromised liver both PCB-126 toxicity and GTE metabolism is altered, with implications of the gut-microbiota in disease risk. The results suggest that there is increased susceptibility to pollutant-induced toxicity for human populations with the end stage of liver disease. Additionally nutritional intervention with beneficial nutrients may be unsuccessful at attenuating disease.

Appendix

OXFORD UNIVERSITY PRESS LICENSE
TERMS AND CONDITIONS
Jun 28, 2019

This Agreement between Jazmyne Barney ("You") and Oxford University Press ("Oxford University Press") consists of your license details and the terms and conditions provided by Oxford University Press and Copyright Clearance Center.

License Number
4617230690302
License date
Jun 27, 2019
Licensed content publisher
Oxford University Press
Licensed content publication
Toxicological Sciences
Licensed content title
Editor’s Highlight: PCB126 Exposure Increases Risk for Peripheral Vascular Diseases in a Liver Injury Mouse Model
Licensed content author
Wahlang, Banrida; Barney, Jazmyne
Licensed content date
Aug 31, 2017
Type of Use
Thesis/Dissertation
Institution name
Title of your work
A compromised liver alters PCB toxicity and nutrient metabolism
Publisher of your work
University of Kentucky
Expected publication date
Jul 2019
Permissions cost
0.00 USD
Value added tax
0.00 USD
Total
0.00 USD
Title
A compromised liver alters PCB toxicity and nutrient metabolism
Institution name
University of Kentucky

Expected presentation date
Jul 2019
Portions
Figure legends for Figures 1, 2, 4 and supplementary figure 1. Rewrite of material and methods, and results and discussion for figures 1, 2, 4, and supplementary figures 1.
Requestor Location
Jazmyne Barney
900 S. Limestone
C.T. Wethington Rm. 589

LEXINGTON, KY 40536
United States
Attn: Jazmyne Barney
Publisher Tax ID
GB125506730
Total
0.00 USD
Terms and Conditions

STANDARD TERMS AND CONDITIONS FOR REPRODUCTION OF MATERIAL FROM AN OXFORD UNIVERSITY PRESS JOURNAL

1. Use of the material is restricted to the type of use specified in your order details.
2. This permission covers the use of the material in the English language in the following territory: world. If you have requested additional permission to translate this material, the terms and conditions of this reuse will be set out in clause 12.
3. This permission is limited to the particular use authorized in (1) above and does not allow you to sanction its use elsewhere in any other format other than specified above, nor does it apply to quotations, images, artistic works etc. that have been reproduced from other sources which may be part of the material to be used.
4. No alteration, omission or addition is made to the material without our written consent. Permission must be re-cleared with Oxford University Press if/when you decide to reprint.
5. The following credit line appears wherever the material is used: author, title, journal, year, volume, issue number, pagination, by permission of Oxford University Press or the sponsoring society if the journal is a society journal. Where a journal is being published on behalf of a learned society, the details of that society must be included in the credit line.
6. For the reproduction of a full article from an Oxford University Press journal for whatever purpose, the corresponding author of the material concerned should be informed of the proposed use. Contact details for the corresponding authors of all Oxford University Press journal contact can be found alongside either the abstract or full text of the article concerned, accessible from

www.oxfordjournals.org Should there be a problem clearing these rights, please contact journals.permissions@oup.com
7. If the credit line or acknowledgement in our publication indicates that any of the figures, images or photos was reproduced, drawn or modified from an earlier source it will be necessary for you to clear this permission with the original publisher as well. If this permission has not been obtained, please note that this material cannot be included in your publication/photocopies.
8. While you may exercise the rights licensed immediately upon issuance of the license at the end of the licensing process for the transaction, provided that you have disclosed complete and accurate details of your proposed use, no license is finally effective unless and until full payment is received from you (either by Oxford University Press or by Copyright Clearance Center (CCC)) as provided in CCC's Billing and Payment terms and conditions. If full payment is not received on a timely basis, then any license preliminarily granted shall be deemed automatically revoked and shall be void as if never granted. Further, in the event that you breach any of these terms and conditions or any of CCC's Billing and Payment terms and conditions, the license is automatically revoked and shall be void as if never granted. Use of materials as described in a revoked license, as well as any use of the materials beyond the scope of an unrevoked license, may constitute copyright infringement and Oxford University Press reserves the right to take any and all action to protect its copyright in the materials.
9. This license is personal to you and may not be sublicensed, assigned or transferred by you to any other person without Oxford University Press's written permission.
10. Oxford University Press reserves all rights not specifically granted in the combination of (i) the license details provided by you and accepted in the course of this licensing transaction, (ii) these terms and conditions and (iii) CCC's Billing and Payment terms and conditions.
11. You hereby indemnify and agree to hold harmless Oxford University Press and CCC, and their respective officers, directors, employs and agents, from and against any and all claims arising out of your use of the licensed material other than as specifically authorized pursuant to this license.
12. Other Terms and Conditions:
v1.4
Questions? customercare@copyright.com or +1-855-239-3415 (toll free in the US) or +1-978-646-2777.

OXFORD UNIVERSITY PRESS LICENSE
TERMS AND CONDITIONS
Jun 28, 2019

This Agreement between Jazmyne Barney ("You") and Oxford University Press

("Oxford University Press") consists of your license details and the terms and conditions provided by Oxford University Press and Copyright Clearance Center.

License Number
4613790169722
License date
Jun 21, 2019
Licensed content publisher
Oxford University Press
Licensed content publication
Toxicological Sciences
Licensed content title
Editor’s Highlight: PCB126 Exposure Increases Risk for Peripheral Vascular Diseases in a Liver Injury Mouse Model
Licensed content author
Wahlang, Banrida; Barney, Jazmyne
Licensed content date
Aug 31, 2017
Type of Use
Thesis/Dissertation
Institution name
Title of your work
The effects of a dysfunctional liver on PCB 126 toxicity and nutrient metabolism
Publisher of your work
University of Kentucky
Expected publication date
Jul 2019
Permissions cost
0.00 USD
Value added tax
0.00 USD
Total
0.00 USD
Title
The effects of a dysfunctional liver on PCB 126 toxicity and nutrient metabolism
Institution name
University of Kentucky
Expected presentation date
Jul 2019
Portions
Figure 1, Figure 2, Figure 4, and Supplementary Figure 1
Requestor Location
Jazmyne Barney
900 S. Limestone
C.T. Wethington Rm. 589

LEXINGTON, KY 40536

United States
Attn: Jazmyne Barney
Publisher Tax ID
GB125506730
Total
0.00 USD
Terms and Conditions

STANDARD TERMS AND CONDITIONS FOR REPRODUCTION OF MATERIAL FROM AN OXFORD UNIVERSITY PRESS JOURNAL

1. Use of the material is restricted to the type of use specified in your order details.
2. This permission covers the use of the material in the English language in the following territory: world. If you have requested additional permission to translate this material, the terms and conditions of this reuse will be set out in clause 12.
3. This permission is limited to the particular use authorized in (1) above and does not allow you to sanction its use elsewhere in any other format other than specified above, nor does it apply to quotations, images, artistic works etc. that have been reproduced from other sources which may be part of the material to be used.
4. No alteration, omission or addition is made to the material without our written consent. Permission must be re-cleared with Oxford University Press if/when you decide to reprint.
5. The following credit line appears wherever the material is used: author, title, journal, year, volume, issue number, pagination, by permission of Oxford University Press or the sponsoring society if the journal is a society journal. Where a journal is being published on behalf of a learned society, the details of that society must be included in the credit line.
6. For the reproduction of a full article from an Oxford University Press journal for whatever purpose, the corresponding author of the material concerned should be informed of the proposed use. Contact details for the corresponding authors of all Oxford University Press journal contact can be found alongside either the abstract or full text of the article concerned, accessible from www.oxfordjournals.org Should there be a problem clearing these rights, please contact journals.permissions@oup.com
7. If the credit line or acknowledgement in our publication indicates that any of the figures, images or photos was reproduced, drawn or modified from an earlier source it will be necessary for you to clear this permission with the original publisher as well. If this permission has not been obtained, please note that this material cannot be included in your publication/photocopies.
8. While you may exercise the rights licensed immediately upon issuance of the license at the end of the licensing process for the transaction, provided that you have disclosed complete and accurate details of your proposed use, no license is finally effective unless and until full payment is received from you (either by Oxford University Press or by Copyright Clearance Center (CCC)) as provided in CCC's Billing and Payment terms and conditions. If full payment is not received

References

1. Hansson, G.K., *Inflammation, atherosclerosis, and coronary artery disease.* N Engl J Med, 2005. **352**(16): p. 1685-95.

2. Koyama, Y. and D.A. Brenner, *Liver inflammation and fibrosis.* J Clin Invest, 2017. **127**(1): p. 55-64.

3. Saltiel, A.R. and J.M. Olefsky, *Inflammatory mechanisms linking obesity and metabolic disease.* J Clin Invest, 2017. **127**(1): p. 1-4.

4. Sheehan, D. and F. Shanahan, *The Gut Microbiota in Inflammatory Bowel Disease.* Gastroenterol Clin North Am, 2017. **46**(1): p. 143-154.

5. Zoller, H. and H. Tilg, *Nonalcoholic fatty liver disease and hepatocellular carcinoma.* Metabolism, 2016. **65**(8): p. 1151-60.

6. Younossi, Z.M., et al., *Changes in the prevalence of the most common causes of chronic liver diseases in the United States from 1988 to 2008.* Clin Gastroenterol Hepatol, 2011. **9**(6): p. 524-530 e1; quiz e60.

7. Chalasani, N., et al., *The diagnosis and management of nonalcoholic fatty liver disease: Practice guidance from the American Association for the Study of Liver Diseases.* Hepatology, 2018. **67**(1): p. 328-357.

8. Sass, D.A., P. Chang, and K.B. Chopra, *Nonalcoholic fatty liver disease: a clinical review.* Dig Dis Sci, 2005. **50**(1): p. 171-80.

9. Younossi, Z.M., et al., *The economic and clinical burden of nonalcoholic fatty liver disease in the United States and Europe.* Hepatology, 2016. **64**(5): p. 1577-1586.

10. Li, L., et al., *Obesity is an independent risk factor for non-alcoholic fatty liver disease: evidence from a meta-analysis of 21 cohort studies.* Obes Rev, 2016. **17**(6): p. 510-9.

11. Bellentani, S., *The epidemiology of non-alcoholic fatty liver disease.* Liver Int, 2017. **37 Suppl 1**: p. 81-84.

12. Argo, C.K. and S.H. Caldwell, *Epidemiology and natural history of non-alcoholic steatohepatitis.* Clin Liver Dis, 2009. **13**(4): p. 511-31.

13. Neuschwander-Tetri, B.A., *Nonalcoholic steatohepatitis and the metabolic syndrome.* Am J Med Sci, 2005. **330**(6): p. 326-35.

14. Angulo, P. and K.D. Lindor, *Non-alcoholic fatty liver disease.* J Gastroenterol Hepatol, 2002. **17 Suppl**: p. S186-90.

15. Buzzetti, E., M. Pinzani, and E.A. Tsochatzis, *The multiple-hit pathogenesis of non-alcoholic fatty liver disease (NAFLD).* Metabolism, 2016. **65**(8): p. 1038-48.

16. Clarke, J.D., et al., *Mechanism of Altered Metformin Distribution in Nonalcoholic Steatohepatitis.* Diabetes, 2015. **64**(9): p. 3305-13.

17. Laho, T., et al., *Effect of nonalcoholic steatohepatitis on renal filtration and secretion of adefovir.* Biochem Pharmacol, 2016. **115**: p. 144-51.

18. Wahlang, B., et al., *Editor's Highlight: PCB126 Exposure Increases Risk for Peripheral Vascular Diseases in a Liver Injury Mouse Model.* Toxicol Sci, 2017. **160**(2): p. 256-267.

19. Wahlang, B., et al., *A compromised liver alters polychlorinated biphenyl-mediated toxicity.* Toxicology, 2017. **380**: p. 11-22.

20. Mouzaki, M., et al., *Intestinal microbiota in patients with nonalcoholic fatty liver disease.* Hepatology, 2013. **58**(1): p. 120-7.

21. Sharpton, T.J., *Role of the Gut Microbiome in Vertebrate Evolution.* mSystems, 2018. **3**(2).

22. Kirpich, I.A., L.S. Marsano, and C.J. McClain, *Gut-liver axis, nutrition, and non-alcoholic fatty liver disease.* Clin Biochem, 2015. **48**(13-14): p. 923-30.

23. Henao-Mejia, J., et al., *Inflammasome-mediated dysbiosis regulates progression of NAFLD and obesity.* Nature, 2012. **482**(7384): p. 179-85.

24. Backhed, F., et al., *Dynamics and Stabilization of the Human Gut Microbiome during the First Year of Life.* Cell Host Microbe, 2015. **17**(5): p. 690-703.

25. Cho, I., et al., *Antibiotics in early life alter the murine colonic microbiome and adiposity.* Nature, 2012. **488**(7413): p. 621-6.

26. David, L.A., et al., *Diet rapidly and reproducibly alters the human gut microbiome.* Nature, 2014. **505**(7484): p. 559-63.

27. Yatsunenko, T., et al., *Human gut microbiome viewed across age and geography.* Nature, 2012. **486**(7402): p. 222-7.

28. Petriello, M.C., et al., *Dioxin-like PCB 126 increases intestinal inflammation and disrupts gut microbiota and metabolic homeostasis.* Environ Pollut, 2018. **242**(Pt A): p. 1022-1032.

29. Boursier, J., et al., *The severity of nonalcoholic fatty liver disease is associated with gut dysbiosis and shift in the metabolic function of the gut microbiota.* Hepatology, 2016. **63**(3): p. 764-75.

30. Yuan, X., et al., *Green Tea Liquid Consumption Alters the Human Intestinal and Oral Microbiome.* Mol Nutr Food Res, 2018. **62**(12): p. e1800178.

31. Lynch, S.V. and O. Pedersen, *The Human Intestinal Microbiome in Health and Disease.* N Engl J Med, 2016. **375**(24): p. 2369-2379.

32. Carpenter, D.O., *Polychlorinated biphenyls (PCBs): routes of exposure and effects on human health.* Rev Environ Health, 2006. **21**(1): p. 1-23.

33. Kampa, M. and E. Castanas, *Human health effects of air pollution.* Environ Pollut, 2008. **151**(2): p. 362-7.

34. Aminov, Z., et al., *Diabetes Prevalence in Relation to Serum Concentrations of Polychlorinated Biphenyl (PCB) Congener Groups and Three Chlorinated Pesticides in a Native American Population.* Environ Health Perspect, 2016. **124**(9): p. 1376-83.

35. Cave, M., et al., *Polychlorinated biphenyls, lead, and mercury are associated with liver disease in American adults: NHANES 2003-2004.* Environ Health Perspect, 2010. **118**(12): p. 1735-42.

36. Crinnion, W.J., *Polychlorinated biphenyls: persistent pollutants with immunological, neurological, and endocrinological consequences.* Altern Med Rev, 2011. **16**(1): p. 5-13.

37. Petriello, M.C., et al., *Relationship between serum trimethylamine N-oxide and exposure to dioxin-like pollutants.* Environ Res, 2018. **162**: p. 211-218.

38. Taylor, K.W., et al., *Evaluation of the association between persistent organic pollutants (POPs) and diabetes in epidemiological studies: a national toxicology program workshop review.* Environ Health Perspect, 2013. **121**(7): p. 774-83.

39. Wahlang, B., et al., *Toxicant-associated steatohepatitis.* Toxicol Pathol, 2013. **41**(2): p. 343-60.

40. Cave, M., et al., *Toxicant-associated steatohepatitis in vinyl chloride workers.* Hepatology, 2010. **51**(2): p. 474-81.

41. Xu, W., X. Wang, and Z. Cai, *Analytical chemistry of the persistent organic pollutants identified in the Stockholm Convention: A review.* Anal Chim Acta, 2013. **790**: p. 1-13.

42. Al-Salman, F. and N. Plant, *Non-coplanar polychlorinated biphenyls (PCBs) are direct agonists for the human pregnane-X receptor and constitutive androstane receptor, and activate target gene expression in a tissue-specific manner.* Toxicol Appl Pharmacol, 2012. **263**(1): p. 7-13.

43. Luthe, G., J.A. Jacobus, and L.W. Robertson, *Receptor interactions by polybrominated diphenyl ethers versus polychlorinated biphenyls: a theoretical Structure-activity assessment.* Environ Toxicol Pharmacol, 2008. **25**(2): p. 202-10.

44. National Toxicology, P., *NTP toxicology and carcinogenesis studies of 3,3',4,4',5-pentachlorobiphenyl (PCB 126) (CAS No. 57465-28-8) in female Harlan Sprague-Dawley rats (Gavage Studies).* Natl Toxicol Program Tech Rep Ser, 2006(520): p. 4-246.

45. Fernandez-Gonzalez, R., et al., *A Critical Review about Human Exposure to Polychlorinated Dibenzo-p-Dioxins (PCDDs), Polychlorinated Dibenzofurans (PCDFs) and Polychlorinated Biphenyls (PCBs) through Foods.* Crit Rev Food Sci Nutr, 2015. **55**(11): p. 1590-617.

46. Lau, J.K., X. Zhang, and J. Yu, *Animal models of non-alcoholic fatty liver disease: current perspectives and recent advances.* J Pathol, 2017. **241**(1): p. 36-44.

47. Vance, D.E., *Role of phosphatidylcholine biosynthesis in the regulation of lipoprotein homeostasis.* Curr Opin Lipidol, 2008. **19**(3): p. 229-34.

48. Yao, Z.M. and D.E. Vance, *Reduction in VLDL, but not HDL, in plasma of rats deficient in choline.* Biochem Cell Biol, 1990. **68**(2): p. 552-8.

49. Corbin, K.D. and S.H. Zeisel, *Choline metabolism provides novel insights into nonalcoholic fatty liver disease and its progression.* Curr Opin Gastroenterol, 2012. **28**(2): p. 159-65.

50. Lu, S.C., *S-Adenosylmethionine.* Int J Biochem Cell Biol, 2000. **32**(4): p. 391-5.

51. Mato, J.M., M.L. Martinez-Chantar, and S.C. Lu, *Methionine metabolism and liver disease.* Annu Rev Nutr, 2008. **28**: p. 273-93.

52. Caballero, F., et al., *Specific contribution of methionine and choline in nutritional nonalcoholic steatohepatitis: impact on mitochondrial S-adenosyl-L-methionine and glutathione.* J Biol Chem, 2010. **285**(24): p. 18528-36.

53. dela Pena, A., et al., *NADPH oxidase is not an essential mediator of oxidative stress or liver injury in murine MCD diet-induced steatohepatitis.* J Hepatol, 2007. **46**(2): p. 304-13.

54. Larter, C.Z. and M.M. Yeh, *Animal models of NASH: getting both pathology and metabolic context right.* J Gastroenterol Hepatol, 2008. **23**(11): p. 1635-48.

55. Baker, N.A., et al., *Coplanar polychlorinated biphenyls impair glucose homeostasis in lean C57BL/6 mice and mitigate beneficial effects of weight loss on glucose homeostasis in obese mice.* Environ Health Perspect, 2013. **121**(1): p. 105-10.

56. Takahashi, Y., et al., *Current pharmacological therapies for nonalcoholic fatty liver disease/nonalcoholic steatohepatitis.* World J Gastroenterol, 2015. **21**(13): p. 3777-85.

57. Wong, V.W., et al., *Pathogenesis and novel treatment options for non-alcoholic steatohepatitis.* Lancet Gastroenterol Hepatol, 2016. **1**(1): p. 56-67.

58. Zhou, J., et al., *Preventive Efficiency of Green Tea and Its Components on Nonalcoholic Fatty Liver Disease.* J Agric Food Chem, 2019. **67**(19): p. 5306-5317.

59. Tan, Y., et al., *Green tea polyphenols ameliorate non-alcoholic fatty liver disease through upregulating AMPK activation in high fat fed Zucker fatty rats.* World J Gastroenterol, 2017. **23**(21): p. 3805-3814.

60. Chung, M.Y., et al., *Green tea extract protects against nonalcoholic steatohepatitis in ob/ob mice by decreasing oxidative and nitrative stress responses induced by proinflammatory enzymes.* J Nutr Biochem, 2012. **23**(4): p. 361-7.

61. Ding, Y., et al., *Epigallocatechin gallate attenuated non-alcoholic steatohepatitis induced by methionine- and choline-deficient diet.* Eur J Pharmacol, 2015. **761**: p. 405-12.

62. Xing, L., et al., *Recent Advances in the Understanding of the Health Benefits and Molecular Mechanisms Associated with Green Tea Polyphenols.* J Agric Food Chem, 2019. **67**(4): p. 1029-1043.

63. Li, J., et al., *Green tea extract provides extensive Nrf2-independent protection against lipid accumulation and NFkappaB pro- inflammatory responses during nonalcoholic steatohepatitis in mice fed a high-fat diet.* Mol Nutr Food Res, 2016. **60**(4): p. 858-70.

64. Li, J., et al., *Green tea extract treatment reduces NFkappaB activation in mice with diet-induced nonalcoholic steatohepatitis by lowering TNFR1 and TLR4 expression and ligand availability.* J Nutr Biochem, 2017. **41**: p. 34-41.

65. Agriculture, U.S.D.o.H.a.H.S.a.U.S.D.o., *2015–2020 Dietary Guidelines for Americans.* 2015(8th Edition).

66. Clemens, R., et al., *Filling America's fiber intake gap: summary of a roundtable to probe realistic solutions with a focus on grain-based foods.* J Nutr, 2012. **142**(7): p. 1390S-401S.

67. Slavin, J., *Fiber and prebiotics: mechanisms and health benefits.* Nutrients, 2013. **5**(4): p. 1417-35.

68. Florowska, A., et al., *Prebiotics as functional food ingredients preventing diet-related diseases.* Food Funct, 2016. **7**(5): p. 2147-55.

69. Chambers, E.S., et al., *The effects of dietary supplementation with inulin and inulin-propionate ester on hepatic steatosis in adults with non-alcoholic fatty liver disease.* Diabetes Obes Metab, 2019. **21**(2): p. 372-376.

70. Boets, E., et al., *Quantification of in Vivo Colonic Short Chain Fatty Acid Production from Inulin.* Nutrients, 2015. **7**(11): p. 8916-29.

71. Javadi, L., et al., *Pro- and prebiotic effects on oxidative stress and inflammatory markers in non-alcoholic fatty liver disease.* Asia Pac J Clin Nutr, 2018. **27**(5): p. 1031-1039.

72. Amato, A., et al., *NAFLD and Atherosclerosis Are Prevented by a Natural Dietary Supplement Containing Curcumin, Silymarin, Guggul, Chlorogenic Acid and Inulin in Mice Fed a High-Fat Diet.* Nutrients, 2017. **9**(5).

73. Perumpail, B.J., et al., *Clinical epidemiology and disease burden of nonalcoholic fatty liver disease.* World J Gastroenterol, 2017. **23**(47): p. 8263-8276.

74. Schecter, A., et al., *Intake of dioxins and related compounds from food in the U.S. population.* J Toxicol Environ Health A, 2001. **63**(1): p. 1-18.

75. Xue, J., et al., *Analysis of NHANES measured blood PCBs in the general US population and application of SHEDS model to identify key exposure factors.* J Expo Sci Environ Epidemiol, 2014. **24**(6): p. 615-21.

76. Park, S.H., et al., *Body burden of persistent organic pollutants on hypertension: a meta-analysis.* Environ Sci Pollut Res Int, 2016. **23**(14): p. 14284-93.

77. Safe, S.H., *Polychlorinated biphenyls (PCBs): environmental impact, biochemical and toxic responses, and implications for risk assessment.* Crit Rev Toxicol, 1994. **24**(2): p. 87-149.

78. Wahlang, B., et al., *Human receptor activation by aroclor 1260, a polychlorinated biphenyl mixture.* Toxicol Sci, 2014. **140**(2): p. 283-97.

79. Oesterling, E., M. Toborek, and B. Hennig, *Benzo[a]pyrene induces intercellular adhesion molecule-1 through a caveolae and aryl hydrocarbon receptor mediated pathway.* Toxicol Appl Pharmacol, 2008. **232**(2): p. 309-16.

80. Pierre, S., et al., *Aryl hydrocarbon receptor-dependent induction of liver fibrosis by dioxin.* Toxicol Sci, 2014. **137**(1): p. 114-24.

81. Vogel, C.F., E. Sciullo, and F. Matsumura, *Activation of inflammatory mediators and potential role of ah-receptor ligands in foam cell formation.* Cardiovasc Toxicol, 2004. **4**(4): p. 363-73.

82. Xiao, L., Z. Zhang, and X. Luo, *Roles of xenobiotic receptors in vascular pathophysiology.* Circ J, 2014. **78**(7): p. 1520-30.

83. Ballestri, S., et al., *Risk of cardiovascular, cardiac and arrhythmic complications in patients with non-alcoholic fatty liver disease.* World J Gastroenterol, 2014. **20**(7): p. 1724-45.

84. Than, N.N. and P.N. Newsome, *A concise review of non-alcoholic fatty liver disease.* Atherosclerosis, 2015. **239**(1): p. 192-202.

85. Hadi, A.M., et al., *Rapid quantification of myocardial fibrosis: a new macro-based automated analysis.* Cell Oncol (Dordr), 2011. **34**(4): p. 343-54.

86. Petriello, M.C., et al., *Dioxin-like pollutants increase hepatic flavin containing monooxygenase (FMO3) expression to promote synthesis of the pro-atherogenic nutrient biomarker trimethylamine N-oxide from dietary precursors.* J Nutr Biochem, 2016. **33**: p. 145-53.

87. Taesuwan, S., et al., *The metabolic fate of isotopically labeled trimethylamine-N-oxide (TMAO) in humans.* J Nutr Biochem, 2017. **45**: p. 77-82.

88. Livak, K.J. and T.D. Schmittgen, *Analysis of relative gene expression data using real-time quantitative PCR and the 2(-Delta Delta C(T)) Method.* Methods, 2001. **25**(4): p. 402-8.

89. Hennig, B., et al., *Proinflammatory properties of coplanar PCBs: in vitro and in vivo evidence.* Toxicol Appl Pharmacol, 2002. **181**(3): p. 174-83.

90. Schlezinger, J.J., et al., *Uncoupling of cytochrome P450 1A and stimulation of reactive oxygen species production by co-planar polychlorinated biphenyl congeners.* Aquat Toxicol, 2006. **77**(4): p. 422-32.

91. Lai, I., et al., *Acute toxicity of 3,3',4,4',5-pentachlorobiphenyl (PCB 126) in male Sprague-Dawley rats: effects on hepatic oxidative stress, glutathione and metals status.* Environ Int, 2010. **36**(8): p. 918-23.

92. Mente, A., et al., *The Relationship Between Trimethylamine-N-Oxide and Prevalent Cardiovascular Disease in a Multiethnic Population Living in Canada.* Can J Cardiol, 2015. **31**(9): p. 1189-94.

93. Ufnal, M., A. Zadlo, and R. Ostaszewski, *TMAO: A small molecule of great expectations.* Nutrition, 2015. **31**(11-12): p. 1317-23.

94. Collins, H.L., et al., *L-Carnitine intake and high trimethylamine N-oxide plasma levels correlate with low aortic lesions in ApoE(-/-) transgenic mice expressing CETP.* Atherosclerosis, 2016. **244**: p. 29-37.

95. Han, S.G., et al., *EGCG protects endothelial cells against PCB 126-induced inflammation through inhibition of AhR and induction of Nrf2-regulated genes.* Toxicol Appl Pharmacol, 2012. **261**(2): p. 181-8.

96. Byrne, C.D. and G. Targher, *NAFLD: a multisystem disease.* J Hepatol, 2015. **62**(1 Suppl): p. S47-64.

97. Tilg, H., P.D. Cani, and E.A. Mayer, *Gut microbiome and liver diseases.* Gut, 2016. **65**(12): p. 2035-2044.

98. Sharpton, S.R., V. Ajmera, and R. Loomba, *Emerging Role of the Gut Microbiome in Nonalcoholic Fatty Liver Disease: From Composition to Function.* Clin Gastroenterol Hepatol, 2018.

99. Newsome, B.J., et al., *Green tea diet decreases PCB 126-induced oxidative stress in mice by up-regulating antioxidant enzymes.* J Nutr Biochem, 2014. **25**(2): p. 126-35.

100. Bruno, R.S., et al., *Green tea extract protects leptin-deficient, spontaneously obese mice from hepatic steatosis and injury.* J Nutr, 2008. **138**(2): p. 323-31.

101. Pan, M.H., et al., *Chemoprevention of nonalcoholic fatty liver disease by dietary natural compounds.* Mol Nutr Food Res, 2014. **58**(1): p. 147-71.

102. Zhou, J., et al., *Preventive Efficiency of Green Tea and Its Components on Nonalcoholic Fatty Liver Disease.* J Agric Food Chem, 2019.

103. Marcolin, E., et al., *Methionine- and choline-deficient diet induces hepatic changes characteristic of non-alcoholic steatohepatitis.* Arq Gastroenterol, 2011. **48**(1): p. 72-9.

104. Machado, M.V., et al., *Correction: Mouse Models of Diet-Induced Nonalcoholic Steatohepatitis Reproduce the Heterogeneity of the Human Disease.* PLoS One, 2015. **10**(6): p. e0132315.

105. Chen, B., et al., *Comparative analysis of fecal phenolic content between normal and obese rats after oral administration of tea polyphenols.* Food Funct, 2018. **9**(9): p. 4858-4864.

106. Nies, A.T. and D. Keppler, *The apical conjugate efflux pump ABCC2 (MRP2).* Pflugers Arch, 2007. **453**(5): p. 643-59.

107. Sookoian, S., et al., *Polymorphisms of MRP2 (ABCC2) are associated with susceptibility to nonalcoholic fatty liver disease.* J Nutr Biochem, 2009. **20**(10): p. 765-70.

108. Hardwick, R.N., et al., *Variations in ATP-binding cassette transporter regulation during the progression of human nonalcoholic fatty liver disease.* Drug Metab Dispos, 2011. **39**(12): p. 2395-402.

109. Hong, J., et al., *Involvement of multidrug resistance-associated proteins in regulating cellular levels of (-)-epigallocatechin-3-gallate and its methyl metabolites.* Biochem Biophys Res Commun, 2003. **310**(1): p. 222-7.

110. Okushio, K., et al., *Methylation of tea catechins by rat liver homogenates.* Biosci Biotechnol Biochem, 1999. **63**(2): p. 430-2.

111. Mannisto, P.T. and S. Kaakkola, *Catechol-O-methyltransferase (COMT): biochemistry, molecular biology, pharmacology, and clinical efficacy of the new selective COMT inhibitors.* Pharmacol Rev, 1999. **51**(4): p. 593-628.

112. Bakir, M.B., et al., *Evaluating the therapeutic potential of one-carbon donors in nonalcoholic fatty liver disease.* Eur J Pharmacol, 2019. **847**: p. 72-82.

113. Meng, X., et al., *Identification and characterization of methylated and ring-fission metabolites of tea catechins formed in humans, mice, and rats.* Chem Res Toxicol, 2002. **15**(8): p. 1042-50.

114. Porras, D., et al., *Protective effect of quercetin on high-fat diet-induced non-alcoholic fatty liver disease in mice is mediated by modulating intestinal microbiota imbalance and related gut-liver axis activation.* Free Radic Biol Med, 2017. **102**: p. 188-202.

115. Ye, J.Z., et al., *Dynamic alterations in the gut microbiota and metabolome during the development of methionine-choline-deficient diet-induced nonalcoholic steatohepatitis.* World J Gastroenterol, 2018. **24**(23): p. 2468-2481.

116. Rau, M., et al., *Fecal SCFAs and SCFA-producing bacteria in gut microbiome of human NAFLD as a putative link to systemic T-cell activation and advanced disease.* United European Gastroenterol J, 2018. **6**(10): p. 1496-1507.

117. van Loo, J., et al., *On the presence of inulin and oligofructose as natural ingredients in the western diet.* Crit Rev Food Sci Nutr, 1995. **35**(6): p. 525-52.

118. Bakhshimoghaddam, F., et al., *Daily Consumption of Synbiotic Yogurt Decreases Liver Steatosis in Patients with Nonalcoholic Fatty Liver Disease: A Randomized Controlled Clinical Trial.* J Nutr, 2018. **148**(8): p. 1276-1284.

119. Sugatani, J., et al., *Dietary inulin alleviates hepatic steatosis and xenobiotics-induced liver injury in rats fed a high-fat and high-sucrose diet: association with the suppression of hepatic cytochrome P450 and hepatocyte nuclear factor 4alpha expression.* Drug Metab Dispos, 2006. **34**(10): p. 1677-87.

120. Sugatani, J., et al., *Effects of dietary inulin, statin, and their co-treatment on hyperlipidemia, hepatic steatosis and changes in drug-metabolizing enzymes in rats fed a high-fat and high-sucrose diet.* Nutr Metab (Lond), 2012. **9**(1): p. 23.

121. Lee, S.M., et al., *TM5441, a plasminogen activator inhibitor-1 inhibitor, protects against high fat diet-induced non-alcoholic fatty liver disease.* Oncotarget, 2017. **8**(52): p. 89746-89760.

122. Yilmaz, Y. and F. Eren, *Serum biomarkers of fibrosis and extracellular matrix remodeling in patients with nonalcoholic fatty liver disease: association with liver histology.* Eur J Gastroenterol Hepatol, 2019. **31**(1): p. 43-46.

123. Henkel, A.S., et al., *Inhibition of Plasminogen Activator Inhibitor 1 Attenuates Hepatic Steatosis but Does Not Prevent Progressive Nonalcoholic Steatohepatitis in Mice.* Hepatol Commun, 2018. **2**(12): p. 1479-1492.

124. Consonni, D., R. Sindaco, and P.A. Bertazzi, *Blood levels of dioxins, furans, dioxin-like PCBs, and TEQs in general populations: a review, 1989-2010.* Environ Int, 2012. **44**: p. 151-62.

125. Pavuk, M., et al., *Serum concentrations of polychlorinated biphenyls (PCBs) in participants of the Anniston Community Health Survey.* Sci Total Environ, 2014. **473-474**: p. 286-97.

126. Petriello, M.C., et al., *Dioxin-like PCB 126 increases systemic inflammation and accelerates atherosclerosis in lean LDL receptor deficient mice.* Toxicol Sci, 2017.

127. Wahlang, B., et al., *Polychlorinated biphenyl exposure alters the expression profile of microRNAs associated with vascular diseases.* Toxicol In Vitro, 2016. **35**: p. 180-7.

128. Wahlang, B., et al., *Evaluation of Aroclor 1260 exposure in a mouse model of diet-induced obesity and non-alcoholic fatty liver disease.* Toxicol Appl Pharmacol, 2014. **279**(3): p. 380-90.

129. Everett, C.J., I. Frithsen, and M. Player, *Relationship of polychlorinated biphenyls with type 2 diabetes and hypertension.* J Environ Monit, 2011. **13**(2): p. 241-51.

130. Perkins, J.T., et al., *Polychlorinated biphenyls and links to cardiovascular disease.* Environ Sci Pollut Res Int, 2016. **23**(3): p. 2160-72.

131. Dumas, M.E., et al., *Metabolic profiling reveals a contribution of gut microbiota to fatty liver phenotype in insulin-resistant mice.* Proc Natl Acad Sci U S A, 2006. **103**(33): p. 12511-6.

132. Mu, Y.P., T. Ogawa, and N. Kawada, *Reversibility of fibrosis, inflammation, and endoplasmic reticulum stress in the liver of rats fed a methionine-choline-deficient diet.* Lab Invest, 2010. **90**(2): p. 245-56.

133. Pan, J.J. and M.B. Fallon, *Gender and racial differences in nonalcoholic fatty liver disease.* World J Hepatol, 2014. **6**(5): p. 274-83.

134. Haro, C., et al., *Intestinal Microbiota Is Influenced by Gender and Body Mass Index.* PLoS One, 2016. **11**(5): p. e0154090.

135. Lonardo, A., et al., *Sex Differences in NAFLD: State of the Art and Identification of Research Gaps.* Hepatology, 2019.

Vita

Jazmyne D'Shario Laurene Barney

Education

2010-2014	University of Cincinnati, Cincinnati, OH
	Major: Bachelor of Science, Chemistry Minor: Africana Studies

Professional Positions Held

2014-2015	Advanced Testing Laboratories, Blue Ash, OH
	Chemical Safety Specialist
2018	Procter and Gamble, Cincinnati, OH
	Regulatory and Product Safety Summer Intern

Research Positions Held

2012-2014	University of Cincinnati Department of Chemistry, Cincinnati, OH
	Undergraduate Research Assistant
2015-present	University of Kentucky Department of Toxicology and Cancer Biology, Lexington, KY
	Graduate Research Assistant

Scholastic and Professional Honors

2010-2014	Choose Ohio First Scholarship, University of Cincinnati, Recipient

2012-2013	Minority Association of Pre-Medical Students, University of Cincinnati, Secretary
2012	Award of Academic Excellence, University of Cincinnati, Recipient
2013-2014	Delta Sigma Theta Sorority Incorporated Zeta Chapter, University of Cincinnati, Recording Secretary
2015-present	Graduate Research Assistantship, University of Kentucky, Recipient
2016-present	University of Kentucky Superfund Research Center, University of Kentucky, Trainee
2017-2019	Biomedical Graduate Student Organization, University of Kentucky, Secretary
2017-2019	Lyman T. Johnson Academic Year Fellowship, University of Kentucky, Recipient
2018	National Institute of Environmental Health Sciences Superfund Research Program Annual Meeting, Sacramento, CA, Graduate Student Poster Winner

Professional Development and Trainings

2017	Webinar-Chemical Safety: Overview of Human Health Risk Assessment, Environmental Protection Agency and University of Kentucky Superfund Research Center
2017	Workshop-University of Kentucky Superfund Statistics Workshop, University of Kentucky
2017	Webinar- Navigating From Job Search through On-Site Interview: Prospective From Hiring Managers and Recruiters, Society of Toxicology
2017	Panelist-HBCU Undergraduate Students Visiting the University of Kentucky Graduate School Student Panel, University of Kentucky

2017	Workshop-University of Kentucky Superfund Scientific Communications Workshop, University of Kentucky
2017	Webinar-Finding Your Dream Job in Regulatory Toxicology, Society of Toxicology
2017-present	Student Member, Society of Toxicology
2017-present	Student Member, American College of Toxicology
2019	Workshop- Risk Assessment Bootcamp, Rutgers University

Poster Abstracts

1. **Barney, J.,** Deng, P., Petriello, M. C., Hoffman, J., Wang, C., Morris, A. J., and Hennig, B. Diet-Induced Steatohepatitis Alters Liver and Gut Microbiota Catalyzed Green Tea Metabolism in Mice. 58th Annual Meeting of the Society of Toxicology, Baltimore, MD; March 2019.

2. **Barney, J.,** Deng, P., Petriello, M. C., Hoffman, J., Wang, C., Morris, A. J., and Hennig, B. Diet-Induced Steatohepatitis Alters Liver and Gut Microbiota Catalyzed Green Tea Metabolism in Mice. 31st Annual Meeting of the NIEHS Superfund Research Program, Sacramento, CA; November 2018.

3. **Barney, J.,** Deng, P., Petriello, M. C., Hoffman, J., Wang, C., Morris, A. J., and Hennig, B. Diet-Induced Steatohepatitis and Inflammation Alters Green Tea Metabolism in Mice. 8th Annual Barnstable Brown Obesity and Diabetes Research Day, Lexington, KY; May 2018.

4. **Barney, J.,** Wahlang, B., Thompson, B., Wang, C., Hamad, O. M., Hoffman, J. B., Petriello, M. C., Morris, A. J., and Hennig, B. Dioxin-like PCB increases peripheral vascular inflammation in mice with liver injury. 30th Annual Meeting of the NIEHS Superfund Research Program, Philadelphia, PA; December 2017.

5. **Barney, J.,** Wahlang, B., Thompson, B., Wang, C., Hamad, O. M., Hoffman, J. B., Petriello, M. C., Morris, A. J., and Hennig, B. PCB 126 Exposure Increases Peripheral Vascular Disease Risk in Mice with Fatty Liver. 50th Annual Cardiovascular Research Day, Lexington, KY; November 2017.

6. **Barney, J.,** Wahlang, B., Thompson, B., Hamad, O., Hoffman, J., Petriello, M., and Hennig, B. The Effects of Polychlorinated Biphenyl 126 on a

Compromised Liver. 56th Annual Meeting of the Society of Toxicology, Baltimore, MD; March 2017.

7. **Barney, J.,** Wahlang, B., Thompson, B., Hamad, O., Hoffman, J., Petriello, M., and Hennig, B. The Effects of Polychlorinated Biphenyl 126 on a Compromised Liver. 12th Annual CCTS Spring Conference, Lexington, KY; April 2017.

8. **Jackson, J.**, McKissic, K., and Mack, J. Diels Alder Reaction in a High Speed Ball Mill. Undergraduate Research Conference, Cincinnati, OH; April 2014.

Publications

1. **Barney, J.,** Deng, P., Petriello, M.C., Hoffman, J., Wang, C., Morris, A.J., and Hennig, B. (2019). Diet-Induced Liver Injury Alters Hepatic and Gut Microbiota Catalyzed Green Tea Metabolism in Mice. (In Prepartation).

2. Deng, P., **Barney, J.**, Petriello, M. C., Morris, A. J., Wahlang, B., and Hennig, B. (2019). Hepatic metabolomics reveals that liver injury increases PCB 126-induced oxidative stress and metabolic dysfunction. *Chemosphere* **217**, 140-149, 10.1016/j.chemosphere.2018.10.196.

3. Petriello, M. C., Brandon, J. A., Hoffman, J., Wang, C., Tripathi, H., Abdel-Latif, A., Ye, X., Li, X., Yang, L., Lee, E., Soman, S., **Barney, J.**, Wahlang, B., Hennig, B., and Morris, A. J. (2017). Dioxin-like PCB 126 increases systemic inflammation and accelerates atherosclerosis in lean LDL receptor deficient mice. *Toxicol Sci* doi: 10.1093/toxsci/kfx275, 10.1093/toxsci/kfx275.

4. Wahlang, B., **Barney, J.**, Thompson, B., Wang, C., Hamad, O. M., Hoffman, J. B., Petriello, M. C., Morris, A. J., and Hennig, B. (2017). Editor's Highlight: PCB126 Exposure Increases Risk for Peripheral Vascular Diseases in a Liver Injury Mouse Model. *Toxicol Sci* **160**(2), 256-267, 10.1093/toxsci/kfx180.